Linear Matrix Inequality Formulation of Spectral Mask Constraints with Applications to FIR Filter Design

Timothy N. Davidson*, Zhi-Quan Luo and Jos F. Sturm

October 2, 2001

Abstract

The design of a finite impulse response (FIR) filter often involves a spectral 'mask' which the magnitude spectrum must satisfy. The mask specifies upper and lower bounds at each frequency, and hence yields an infinite number of constraints. In current practice, spectral masks are often approximated by discretization, but in this paper we will derive a result which allows us to precisely enforce piecewise constant and piecewise trigonometric polynomial masks in a finite and convex manner via linear matrix inequalities. While this result is theoretically satisfying in that it allows us to avoid the heuristic approximations involved in discretization techniques, it is also of practical interest because it generates competitive design algorithms (based on interior point methods) for a diverse class of FIR filtering and narrowband beamforming problems. The examples we provide include the design of standard linear and nonlinear phase FIR filters, robust 'chip' waveforms for wireless communications, and narrowband beamformers for linear antenna arrays. Our main result also provides a contribution to system theory, as it is an extension of the well-known Positive-Real and Bounded-Real Lemmas.

Keywords: FIR digital filter design; beamforming; spectral masks; optimization
SP-EDICS: 2–FILT

This research was supported in part by the Natural Sciences and Engineering Research Council of Canada, Grant No. OPG0090391. The second author is also supported by the Canada Research Chair program. The third author was also supported by travel grant R46-415 of the Netherlands Organization for Scientific Research (NWO).

*Corresponding author. Department of Electrical and Computer Engineering, McMaster University, 1280 Main Street West, Hamilton, Ontario, L8S 4K1, Canada. Tel: +1-905-525-9140, Ext. 27352. Fax: +1-905-521-2922. Email: `davidson@mcmaster.ca`

T. N. Davidson and Z.-Q. Luo are with the Department of Electrical and Computer Engineering, McMaster University, Hamilton, Ontario, L8S 4K1, Canada.

J. F. Sturm is with the Department of Econometrics, Tilburg University, 5000 LE, Tilburg, The Netherlands.

I. Introduction

In the design of finite impulse response (FIR) filters, one often encounters a spectral mask constraint on the magnitude of the frequency response of the filter (e.g., [1–4]). That is, for given $L(e^{\mathrm{j}\omega})$ and $U(e^{\mathrm{j}\omega})$, constrain the (possibly complex) filter coefficients g_k so that

$$L(e^{\mathrm{j}\omega}) \leq |G(e^{\mathrm{j}\omega})| \leq U(e^{\mathrm{j}\omega}) \qquad \text{for all } 0 \leq \omega < 2\pi, \tag{1}$$

or determine that the constraint cannot be satisfied. Here, $\mathrm{j} = \sqrt{-1}$ and $G(e^{\mathrm{j}\omega}) = \sum_k g_k e^{-\mathrm{j}\omega k}$ is the frequency response of the filter. A spectral mask constraint can be rather awkward to accommodate into general optimization-based filter design techniques for two reasons. First, it is semi-infinite in the sense that there are two inequality constraints for every $\omega \in [0, 2\pi)$. Second, the set of feasible filter coefficients is in general non-convex due to the lower bound on $|G(e^{\mathrm{j}\omega})|$. In order to efficiently solve filter design problems employing such constraints, we must find a way in which (1) can be represented in a finite and convex manner.

There are two established approaches [1] to deal with the problem of non-convexity of (1). The first is to enforce additional constraints on the parameters g_k so that $G(e^{\mathrm{j}\omega})$ has 'linear phase'. In that case $|G(e^{\mathrm{j}\omega})|$ becomes a linear function of approximately half the g_k's (the rest are determined via the linear phase constraint), and hence (1) can be reduced to two semi-infinite linear (and hence convex) constraints. However, phase linearity may be an excessively restrictive constraint in some applications [5]. The second approach to deal with non-convexity is to reformulate (1) in terms of the autocorrelation of the filter [5–10]. In particular, if $r_m = \sum_k g_k \bar{g}_{k-m}$ represents the autocorrelation of the filter, then $R(e^{\mathrm{j}\omega}) = |G(e^{\mathrm{j}\omega})|^2$, and hence (1) is equivalent to

$$L(e^{\mathrm{j}\omega})^2 \leq R(e^{\mathrm{j}\omega}) \leq U(e^{\mathrm{j}\omega})^2 \qquad \text{for all } 0 \leq \omega < 2\pi, \tag{2}$$

which amounts to two semi-infinite linear constraints on r_m. (Observe that $r_{-m} = \bar{r}_m$ and hence $R(e^{\mathrm{j}\omega})$ is real.) Hence, by reformulating the mask constraint in terms of r_m, $m \geq 0$, we obtain convex constraints. Note that the constraint that $R(e^{\mathrm{j}\omega}) \geq L(e^{\mathrm{j}\omega})^2 \geq 0$ is sufficient to ensure that a filter g_k can be extracted (though not uniquely) from a designed autocorrelation r_m via spectral factorization [9, 11].

The problem of representing (1) or (2) in a finite manner is more challenging. (For simplicity we will phrase our discussion in terms of (2).) One standard, but ad-hoc, approach is to approximate the constraints by discretizing them uniformly in frequency and enforcing the $2N$ linear constraints

$$L(e^{\mathrm{j}\omega_i})^2 + \epsilon \leq R(e^{\mathrm{j}\omega_i}) \leq U(e^{\mathrm{j}\omega_i})^2 - \epsilon \qquad \text{for } \omega_i = 2\pi i/N,\ i = 0, 1, \ldots, N-1, \tag{3}$$

where N and ϵ are chosen heuristically. For a fixed N, one must choose ϵ to be small enough so that the over-constraining of the problem at frequencies ω_i does not result in significant performance loss, yet one must choose ϵ to be large enough for satisfaction of (3) to guarantee satisfaction of (2) for all $0 \leq \omega < 2\pi$. Unfortunately, as N is increased so that ϵ can be reduced, the resulting formulation can become prone to numerical difficulties. In practice, N and ϵ are usually chosen according to engineering 'rules of thumb' that depend on the design problem at hand. (Other discretization techniques are also available [12, 13].) For certain design problems, algorithms of the exchange type [1, 3, 4] offer an alternative to direct discretization techniques. These methods employ a non-uniform discretization of (2) at each stage of the algorithm, where the sample points are determined by the stationary points of the current estimate of the optimal $R(e^{j\omega})$, and any points of discontinuity in the mask. (In practice, the stationary points are often approximated using fine uniform discretization [4].) At each stage of the algorithm an optimization problem is solved subject to appropriate equality constraints derived from (2) at those sample points. Although exchange methods often work well for the design of low-pass filters, substantial effort is required to guarantee the algorithm's convergence [4]. Furthermore, the algorithms may require substantial 're-tailoring' in order to incorporate additional constraints on the filter coefficients (e.g., [14]). Recently, a precise finite representation of (2) that does not require discretization was developed using dual parameterization methods [15]. However, that representation may result in non-convex design problems.

In this paper, we derive a precise finite representation of a large class of spectral mask constraints that results in convex design problems. This representation provides a theoretically satisfying characterization of the mask constraint that avoids the heuristic approximation of discretization techniques, yet generates practically competitive design algorithms. Our development begins with the derivation of a (finite) linear matrix inequality (LMI) characterization of the set of trigonometric polynomials of a given order whose real part is positive over a given segment of the unit circle (Theorem 3). While that result is a contribution to system theory in itself (as outlined below), we also show that it allows us to precisely enforce piecewise constant and piecewise trigonometric polynomial spectral masks in a convex and finite manner. As a result, these masks can be incorporated, without approximation, into the diverse class of FIR filter and narrowband beamformer design problems which can be efficiently solved using well-established interior point methods (e.g., [8–10]). We will provide examples which show how our main result leads to effective algorithms for peak-constrained weighted least-squares design of linear-phase and nonlinear-phase FIR filters, for the design of robust 'chip' waveforms for digital wireless communication systems based on code division multiple access, and for the design of narrowband beamformers for linear antenna arrays with uncertain signal and interference directions.

Our main theoretical result (Theorem 3) provides an LMI characterization of the set of trigonometric polynomials whose real part is positive over a segment of the unit circle. When specialized to the case where the segment is the whole circle, this result generates a new LMI formulation of the Positive Real Lemma [16, 17] (and the closely related Kalman-Yakubovich-Popov [KYP] Lemma) for FIR systems. This new formulation states that for r_m, $-M+1 \leq m \leq M-1$, with $r_{-m} = \bar{r}_m$, $R(e^{\mathrm{j}\omega}) \geq 0$ for all $\omega \in [0, 2\pi]$ if and only if there exists an $M \times M$ positive semidefinite Hermitian matrix $\boldsymbol{X}$ such that $\mathrm{tr}(\boldsymbol{X}) = r_0$ and $\sum_{\ell=0}^{M-1-m} [\boldsymbol{X}]_{\ell+m,\ell} = r_m$, for $1 \leq m \leq M-1$. (For later notational convenience, we will index the elements of vectors and matrices starting from zero.) However, Theorem 3 generates LMI formulations of more general constraints of the form $R(e^{\mathrm{j}\omega}) \geq \mathrm{Re}\ A(e^{\mathrm{j}\omega})$ for all $\omega \in [\alpha, \beta]$, or for all $\omega \in [0, 2\pi) \setminus (\alpha, \beta)$, where $A(e^{\mathrm{j}\omega}) = \sum_{k=0}^{M_A-1} a_k e^{-\mathrm{j}\omega k}$ is a trigonometric polynomial and $\mathrm{Re} \cdot$ denotes the real part. Since these LMI formulations apply to segments of the unit circle and naturally incorporate non-constant lower bounds, they can be considered as generalizations of the Positive Real Lemma. Theorem 3 also generates LMI formulations of constraints of the form $R(e^{\mathrm{j}\omega}) \leq \mathrm{Re}\ B(e^{\mathrm{j}\omega})$ for all $\omega \in [\alpha, \beta]$, or for all $\omega \in [0, 2\pi) \setminus (\alpha, \beta)$, which can be considered as generalizations of the Bounded Real Lemma [18].

Our notational conventions are as follows: Vectors and matrices will be represented by bold lowercase and uppercase letters, respectively. The elements of these structures will be indexed starting from zero and will be denoted by medium weight lower case letters with appropriate subscripts; e.g., $g_k = [\boldsymbol{g}]_k$ and $x_{ij} = [\boldsymbol{X}]_{ij}$. Operators will be represented by bold uppercase letters in a sans-serif font. In order to illuminate the connections between the results for polynomials on the real line and trigonometric polynomials on the unit circle, we define

$$\boldsymbol{u}(t;n) := \begin{bmatrix} 1 & t & t^2 & \cdots & t^n \end{bmatrix}^{\mathrm{T}}, \quad \boldsymbol{v}(\theta;n) := \begin{bmatrix} 1 & e^{\mathrm{j}\theta} & e^{\mathrm{j}2\theta} & \cdots & e^{\mathrm{j}n\theta} \end{bmatrix}^{\mathrm{T}}, \tag{4}$$

where the superscript "T" denotes the transpose (without conjugation). Thus, the components of $\boldsymbol{u}(t;n)$ form a basis of the (real) function space of polynomials of degree n on the real line, whereas the components of $\boldsymbol{v}(\theta;n)$ form a basis of the (complex) function space of trigonometric polynomials of degree n on $[0, 2\pi)$. Consequently, an nth order polynomial $p(t) = \sum_{k=0}^{n} p_k t^k$ can be written as $p(t) = \boldsymbol{u}(t;n)^{\mathrm{T}}\boldsymbol{p}$, where $[\boldsymbol{p}]_k = p_k$. Similarly, if the sequence g_k denotes the impulse response of a causal FIR filter, and if $[\boldsymbol{g}]_k = g_k$, then the frequency response $G(e^{\mathrm{j}\theta}) = \sum_{k=0}^{n} g_k e^{-\mathrm{j}k\theta} = \boldsymbol{v}(\theta;n)^{\mathrm{H}}\boldsymbol{g}$, where the superscript "H" denotes the Hermitian transpose. The (complex valued) inner product between two complex matrices $\boldsymbol{X}$ and $\boldsymbol{Z}$ is defined as

$$\langle \boldsymbol{X}, \boldsymbol{Z} \rangle = \mathrm{tr}\ \boldsymbol{X}^{\mathrm{H}}\boldsymbol{Z}. \tag{5}$$

We shall denote by $\mathcal{H}_+^{n\times n}$ the set of $n \times n$ positive semidefinite (complex) Hermitian matrices, and by $\mathcal{S}_+^{n\times n}$ the subset of $\mathcal{H}_+^{n\times n}$ consisting of the real symmetric positive semidefinite matrices. For a complex number $x \in \mathbb{C}$, we denote the polar coordinates as $(|x|, \arg x) \in \mathbb{R}_+ \times [0, 2\pi)$, i.e. $x = |x|e^{\mathrm{j}\arg x}$, with $\arg x \in [0, 2\pi)$.

II. Transformation of Polynomial Basis

In this section, we establish a one-to-one correspondence between polynomials of degree $2n$ on the real line, and trigonometric polynomials of degree n on $(0, 2\pi)$, where the coefficients of the trigonometric polynomials may be complex numbers. The main result of this section is stated in Theorem 1, but we first state some intermediate results.

By a result from classical complex analysis [19], the complex exponential function $e^{\mathrm{j}\theta}$ can be represented as a (complex) rational function of t over the real line:

$$e^{\mathrm{j}\theta} = \frac{t+\mathrm{j}}{t-\mathrm{j}} = \frac{(t+\mathrm{j})^2}{1+t^2}.$$

This mapping from $t \in (-\infty, \infty)$ to $\theta \in (0, 2\pi)$ is one-to-one. In fact, it is a conformal mapping and is closely related to the 'bilinear transform' which is used to map the left half plane to the unit disc in the standard transformation of analog filter designs into the discrete-time domain [20]. This mapping provides the basis for relating the polynomials over the real line with trigonometric polynomials over the unit circle. The following lemma further relates an arbitrary power of $e^{\mathrm{j}\theta}$ to a rational function of t.

Lemma 1: Let $\theta \in (0, 2\pi)$ and $t \in \mathbb{R}$ be related by

$$e^{\mathrm{j}\theta} = \frac{(t+\mathrm{j})^2}{1+t^2}.$$

Then for any positive integer $i \geq 1$, we have

$$e^{\mathrm{j}i\theta} = \frac{1}{(1+t^2)^i}\left(\sum_{k=0}^{i}(-1)^k\binom{2i}{2k}t^{2(i-k)} + \mathrm{j}\sum_{k=0}^{i-1}(-1)^k\binom{2i}{2k+1}t^{2(i-k)-1}\right).$$

Proof. This is a simple application of Newton's binomial formula. **Q.E.D.**

Let us define a lower triangular matrix $\boldsymbol{G}(n)$ of size $(n+1)\times(n+1)$ whose (i,j)-th entry is given by

$$g_{ij}(n) := \begin{cases} 0, & \text{for } 0 \leq i \leq j-1, \\ \binom{n-j}{n-i}, & \text{for } j \leq i \leq n. \end{cases} \tag{6}$$

Notice that the diagonal entries of $\boldsymbol{G}(n)$ are equal to 1, hence, it is invertible. We shall denote the columns of $\boldsymbol{G}(n)$ by $\boldsymbol{g}_j(n)$, $j = 0, 1, ..., n$. In addition, for each $0 \leq k \leq n$, we define a $(n+1)\times(n+1)$ matrix $\boldsymbol{H}(k;n)$ whose (i,j)-th entry is given by

$$h_{ij}(k;n) := \begin{cases} \binom{n-j}{n-i-k}, & \text{for } k \leq j \leq n,\ j-k \leq i \leq n-k, \\ 0, & \text{otherwise.} \end{cases} \tag{7}$$

We shall denote the j-th column of this matrix by $\boldsymbol{h}_j(k;n)$. Obviously, we have $\boldsymbol{H}(0;n) = \boldsymbol{G}(n)$. We remark that

$$\boldsymbol{u}(x;n)^{\mathrm{T}}\boldsymbol{h}_j(k;n) = \sum_{i=j-k}^{n-k}\binom{n-j}{n-i-k}x^i = x^{j-k}\sum_{\ell=0}^{n-j}\binom{n-j}{n-j-\ell}x^\ell = x^{j-k}(1+x)^{n-j}. \tag{8}$$

Based on (8), we can now restate Lemma 1 as follows.

Lemma 2: Let $\theta \in (0, 2\pi)$ and $t \in \mathbb{R}$ be related by

$$e^{\mathrm{j}\theta} = \frac{(t+\mathrm{j})^2}{1+t^2}.$$

Then

$$1 = e^{\mathrm{j}0\theta} = \frac{\boldsymbol{u}(t^2;n)^{\mathrm{T}}\boldsymbol{f}_0}{(1+t^2)^n},$$

and

$$e^{\mathrm{j}\ell\theta} = \frac{\boldsymbol{u}(t^2;n)^{\mathrm{T}}\boldsymbol{f}_\ell + \mathrm{j}t(\boldsymbol{u}(t^2;n-1)^{\mathrm{T}}\tilde{\boldsymbol{f}}_{\ell-1})}{(1+t^2)^n}, \qquad \ell = 1, 2, \dots, n,$$

where

$$\boldsymbol{f}_\ell := \sum_{k=0}^{\ell} (-1)^k \binom{2\ell}{2k} \boldsymbol{h}_\ell(k;n), \qquad \ell = 0, 1, \dots, n, \tag{9}$$

and

$$\tilde{\boldsymbol{f}}_\ell := \sum_{k=0}^{\ell} (-1)^k \binom{2(\ell+1)}{2k+1} \boldsymbol{h}_\ell(k;n-1), \qquad \ell = 0, 1, \dots, n-1. \tag{10}$$

Proof. The proof follows directly from Lemma 1 and the definitions of $\boldsymbol{f}_\ell$ and $\tilde{\boldsymbol{f}}_\ell$. **Q.E.D.**

Now, consider the elementary identities

$$\binom{n-1}{m} = \frac{n-m}{n}\binom{n}{m}, \quad \binom{n-1}{m-1} = \frac{m}{n}\binom{n}{m}, \quad \binom{n-1}{n-1} = \binom{n}{n} = 1,$$

which are valid for any $m = 0, 1, \dots, n-1$. An immediate consequence of the above identities and (7) is that

$$\boldsymbol{h}_j(k;n) + \boldsymbol{h}_j(k-1;n) = \boldsymbol{h}_{j-1}(k-1;n). \tag{11}$$

Alternatively, the above identity can be established from (8). Since $\boldsymbol{h}_j(0;n) = \boldsymbol{g}_j(n)$, a simple induction argument shows that

$$\boldsymbol{h}_j(k;n) \in \text{ span}\,\{\boldsymbol{g}_0(n), \boldsymbol{g}_1(n), \dots, \boldsymbol{g}_j(n)\}. \tag{12}$$

The following lemma further strengthens the above relation.

Lemma 3: There holds that

$$(-1)^k \boldsymbol{h}_j(k;n) - \boldsymbol{g}_j(n) \in \text{ span}\,\{\boldsymbol{g}_0(n), \boldsymbol{g}_1(n), \dots, \boldsymbol{g}_{j-1}(n)\}. \tag{13}$$

Proof. For a given j, let $\boldsymbol{w}(k) = (-1)^k \boldsymbol{h}_j(k;n) - \boldsymbol{g}_j(n)$. We will prove the lemma by induction on k.

For $k = 0$, we have $\boldsymbol{w}(0) = \boldsymbol{h}_j(0;n) - \boldsymbol{g}_j(n) = \boldsymbol{g}_j(n) - \boldsymbol{g}_j(n) = 0$, so (13) holds trivially. Consider now a $k \in \{1, 2, \ldots, j\}$, and make the hypothesis that $\boldsymbol{w}(k-1) \in \text{ span}\,\{\boldsymbol{g}_0(n), \boldsymbol{g}_1(n), \ldots, \boldsymbol{g}_{j-1}(n)\}$. We have

$$\begin{aligned}\boldsymbol{w}(k) = (-1)^k \boldsymbol{h}_j(k;n) - \boldsymbol{g}_j(n) &= (-1)^k \big(\boldsymbol{h}_j(k;n) + \boldsymbol{h}_j(k-1;n)\big) + (-1)^{k-1}\boldsymbol{h}_j(k-1;n) - \boldsymbol{g}_j(n) \\ &= (-1)^k \boldsymbol{h}_{j-1}(k-1;n) + (-1)^{k-1}\boldsymbol{h}_j(k-1;n) - \boldsymbol{g}_j(n) \\ &= (-1)^k \boldsymbol{h}_{j-1}(k-1;n) + \boldsymbol{w}(k-1).\end{aligned}$$

By (12), we know that

$$\boldsymbol{h}_{j-1}(k-1;n) \in \text{ span}\,\{\boldsymbol{g}_0(n), \boldsymbol{g}_1(n), \ldots, \boldsymbol{g}_{j-1}(n)\}.$$

Hence if $\boldsymbol{w}(k-1) \in \text{ span}\,\{\boldsymbol{g}_0(n), \boldsymbol{g}_1(n), \ldots, \boldsymbol{g}_{j-1}(n)\}$ then $\boldsymbol{w}(k) \in \text{ span}\,\{\boldsymbol{g}_0(n), \boldsymbol{g}_1(n), \ldots, \boldsymbol{g}_{j-1}(n)\}$. Since $\boldsymbol{w}(0)$ satisfies (13), a simple induction argument completes the proof. **Q.E.D.**

Now we can substitute (13) into the expressions (9)–(10) to obtain the following relations:

$$\boldsymbol{f}_j - \left(\sum_{k=0}^{j} \binom{2j}{2k}\right) \boldsymbol{g}_j(n) \in \text{ span}\,\{\boldsymbol{g}_0(n), \boldsymbol{g}_1(n), \ldots, \boldsymbol{g}_{j-1}(n)\},$$

and

$$\tilde{\boldsymbol{f}}_j - \left(\sum_{k=0}^{j} \binom{2(j+1)}{2k+1}\right) \boldsymbol{g}_j(n-1) \in \text{ span}\,\{\boldsymbol{g}_0(n-1), \boldsymbol{g}_1(n-1), \ldots, \boldsymbol{g}_{j-1}(n-1)\}.$$

As a result, we have that

$$\text{span}\,\{\boldsymbol{f}_0, \boldsymbol{f}_1, \ldots, \boldsymbol{f}_j\} = \text{ span}\,\{\boldsymbol{g}_0(n), \boldsymbol{g}_1(n), \ldots, \boldsymbol{g}_j(n)\}, \quad \text{for } j = 0, 1, \ldots, n,$$

and

$$\text{span}\,\{\tilde{\boldsymbol{f}}_0, \tilde{\boldsymbol{f}}_1, \ldots, \tilde{\boldsymbol{f}}_j\} = \text{ span}\,\{\boldsymbol{g}_0(n-1), \boldsymbol{g}_1(n-1), \ldots, \boldsymbol{g}_j(n-1)\}, \quad \text{for } j = 0, 1, \ldots, n-1.$$

This implies that the matrices

$$\boldsymbol{F} = \begin{bmatrix} \boldsymbol{f}_0, & \boldsymbol{f}_1, & \ldots, & \boldsymbol{f}_n \end{bmatrix} \quad \text{and} \quad \tilde{\boldsymbol{F}} = \begin{bmatrix} \tilde{\boldsymbol{f}}_0, & \tilde{\boldsymbol{f}}_1, & \ldots, & \tilde{\boldsymbol{f}}_{n-1} \end{bmatrix}$$

must be invertible. In light of Lemma 2, this establishes an one-to-one correspondence between polynomials of degree $2n$ on the real line, and trigonometric polynomials of degree n on $(0, 2\pi)$. We summarize the result in the following theorem.

Theorem 1: The mapping $\eta(t) := \arg((t+\mathrm{j})^2/(1+t^2))$ is a bijection between $\mathbb{R}$ and $(0, 2\pi)$. In particular, the inverse function $\eta^{-1}(\theta)$ for $\theta \in (0, 2\pi)$ is given by

$$\eta^{-1}(\theta) = \frac{\sin\theta}{1-\cos\theta}.$$

Furthermore, for any vector $\boldsymbol{p} \in \mathbb{R}^{2n+1}$ there exists a vector $\boldsymbol{c} \in \mathbb{R}^{2n+1}$ such that

$$\frac{\sum_{i=0}^{2n} p_i t^i}{(1+t^2)^n} = \mathrm{Re}\left(c_0 + \sum_{k=1}^{n}(c_{2k} - \mathrm{j}c_{2k-1})e^{\mathrm{j}k\eta(t)}\right), \quad \text{for all } t \in \mathbb{R}.$$

Conversely, for any vector $\boldsymbol{c} \in \mathbb{R}^{2n+1}$ there exists a vector $\boldsymbol{p} \in \mathbb{R}^{2n+1}$ such that

$$\frac{\sum_{i=0}^{2n} p_i(\eta^{-1}(\theta))^i}{(1+(\eta^{-1}(\theta))^2)^n} = \mathrm{Re}\left(c_0 + \sum_{k=1}^{n}(c_{2k} - \mathrm{j}c_{2k-1})e^{\mathrm{j}k\theta}\right), \quad \text{for all } \theta \in (0, 2\pi).$$

Proof. The bijectivity of $\eta(t)$ follows from simple calculus. The remaining part of the theorem is due to the invertibility of $\boldsymbol{F}$ and $\tilde{\boldsymbol{F}}$. **Q.E.D.**

III. Characterization of Nonnegative Polynomials on a Segment

In this section we characterize the set of trigonometric polynomials which are non-negative over a segment of the unit circle. The main result will be stated in Theorem 2, but first we state some preliminary results. We begin with a review of a well known characterization [21, 22] of non-negative polynomials over a line segment in $\mathbb{R}$. We refer to Powers and Reznick [23] for a recent survey on characterizations for polynomials that are non-negative on an interval.

Proposition 1 (Markov-Lukacs) Let $\boldsymbol{p} \in \mathbb{R}^{2n+1}$ and $a, b \in \mathbb{R}$, $a < b$. Then

$$\boldsymbol{u}(t; 2n)^{\mathrm{T}}\boldsymbol{p} \geq 0 \text{ for all } t \in [a, b]$$

if and only if there exist $\boldsymbol{q} \in \mathbb{R}^{n+1}$ and $\boldsymbol{r} \in \mathbb{R}^n$ such that

$$\boldsymbol{u}(t; 2n)^{\mathrm{T}}\boldsymbol{p} = \big(\boldsymbol{u}(t; n)^{\mathrm{T}}\boldsymbol{q}\big)^2 + (t-a)(b-t)\big(\boldsymbol{u}(t; n-1)^{\mathrm{T}}\boldsymbol{r}\big)^2.$$

Moreover, it holds that

$$\boldsymbol{u}(t; 2n)^{\mathrm{T}}\boldsymbol{p} \geq 0 \text{ for all } t \in [a, \infty)$$

if and only if there exist $\boldsymbol{q} \in \mathbb{R}^{n+1}$ and $\boldsymbol{r} \in \mathbb{R}^n$ such that

$$\boldsymbol{u}(t; 2n)^{\mathrm{T}}\boldsymbol{p} = \big(\boldsymbol{u}(t; n)^{\mathrm{T}}\boldsymbol{q}\big)^2 + (t-a)\big(\boldsymbol{u}(t; n-1)^{\mathrm{T}}\boldsymbol{r}\big)^2.$$

The following corollary of Proposition 1 provides a characterization for polynomials which are non-negative over the complement of a finite symmetric interval in $\mathbb{R}$.

Corollary 1: Let $\boldsymbol{p} \in \mathbb{R}^{2n+1}$ and let $a > 0$ be a given positive number. Then

$$\boldsymbol{u}(t; 2n)^{\mathrm{T}}\boldsymbol{p} \geq 0 \text{ for all } t \notin (-a, a)$$

if and only if there exist $\boldsymbol{q} \in \mathbb{R}^{n+1}$ and $\boldsymbol{r} \in \mathbb{R}^n$ such that

$$\boldsymbol{u}(t;2n)^{\mathrm{T}}\boldsymbol{p} = \big(\boldsymbol{u}(t;n)^{\mathrm{T}}\boldsymbol{q}\big)^2 + (t^2 - a^2)\big(\boldsymbol{u}(t;n-1)^{\mathrm{T}}\boldsymbol{r}\big)^2.$$

Proof. Let $\tilde{p}_i := p_{2n-i}$ for $i = 0, 1, \ldots, 2n$. Then for $t \neq 0$ we have

$$\boldsymbol{u}(t;2n)^{\mathrm{T}}\boldsymbol{p} = t^{2n}\big(\boldsymbol{u}(1/t;2n)^{\mathrm{T}}\tilde{\boldsymbol{p}}\big).$$

Since $t^2 \geq a^2 > 0$ for all $t \notin (-a, a)$, it follows that

$$\boldsymbol{u}(t;2n)^{\mathrm{T}}\boldsymbol{p} \geq 0 \quad \text{for all } t \notin (-a, a)$$

if and only if

$$\boldsymbol{u}(s;2n)^{\mathrm{T}}\tilde{\boldsymbol{p}} \geq 0 \quad \text{for all } s \in [-1/a, 1/a].$$

By Proposition 1, the above relation holds if and only if there exist $\tilde{\boldsymbol{q}} \in \mathbb{R}^{n+1}$ and $\tilde{\boldsymbol{r}} \in \mathbb{R}^n$ such that

$$\boldsymbol{u}(s;2n)^{\mathrm{T}}\tilde{\boldsymbol{p}} = \big(\boldsymbol{u}(s;n)^{\mathrm{T}}\tilde{\boldsymbol{q}}\big)^2 + \frac{1 - a^2 s^2}{a^2}\big(\boldsymbol{u}(s;n-1)^{\mathrm{T}}\tilde{\boldsymbol{r}}\big)^2.$$

Letting

$$q_i := \tilde{q}_{n-i} \ \text{ and } \ r_i := \tilde{r}_{n-1-i}/a, \quad \text{for } i = 0, 1, \ldots, n,$$

proves the result. **Q.E.D.**

The next corollary further extends Corollary 1 to the case where the interval is non-symmetric.

Corollary 2: Let $\boldsymbol{p} \in \mathbb{R}^{2n+1}$ and $a, b \in \mathbb{R}$, $a < b$. Then

$$\boldsymbol{u}(t;2n)^{\mathrm{T}}\boldsymbol{p} \geq 0 \text{ for all } t \notin (a, b) \tag{14}$$

if and only if there exist $\boldsymbol{q} \in \mathbb{R}^{n+1}$ and $\boldsymbol{r} \in \mathbb{R}^n$ such that

$$\boldsymbol{u}(t;2n)^{\mathrm{T}}\boldsymbol{p} = \big(\boldsymbol{u}(t;n)^{\mathrm{T}}\boldsymbol{q}\big)^2 + (t-a)(t-b)\big(\boldsymbol{u}(t;n-1)^{\mathrm{T}}\boldsymbol{r}\big)^2. \tag{15}$$

Proof. It is obvious that (15) implies (14). Suppose now that (14) holds. Let us define

$$s := 2t - (a+b), \quad \tilde{a} := b - a.$$

It is clear (e.g., from Newton's binomial formula) that there exists $\tilde{\boldsymbol{p}} \in \mathbb{R}^{n+1}$ such that

$$\boldsymbol{u}(t;2n)^{\mathrm{T}}\boldsymbol{p} = \boldsymbol{u}(2t-(a+b);2n)^{\mathrm{T}}\tilde{\boldsymbol{p}} = \boldsymbol{u}(s;2n)^{\mathrm{T}}\tilde{\boldsymbol{p}}.$$

Since $(s^2 - \tilde{a}^2) = 4(t-a)(t-b)$, Corollary 1 implies that (15) holds for some $\boldsymbol{q} \in \mathbb{R}^{n+1}$ and $\boldsymbol{r} \in \mathbb{R}^n$. **Q.E.D.**

The next lemma determines a simple trigonometric polynomial which is non-negative over a given segment of the unit circle but is non-positive over its complement. In particular, given $\alpha,\ \beta \in [0, 2\pi)$, we define a vector $\boldsymbol{d}(\alpha, \beta) \in \mathbb{R} \times \mathbb{C}$ as follows:

$$\boldsymbol{d}(\alpha,\beta) := \begin{cases} \begin{bmatrix} \cos\alpha + \cos\beta - \cos(\beta-\alpha) - 1 \\ (1-e^{\mathrm{j}\alpha})(e^{\mathrm{j}\beta}-1) \end{bmatrix} & \text{if } \alpha > 0 \\ \begin{bmatrix} -\sin\beta \\ \mathrm{j}(1-e^{\mathrm{j}\beta}) \end{bmatrix} & \text{if } \alpha = 0. \end{cases} \tag{16}$$

We remark that

$$\boldsymbol{d}(0,\beta) = \lim_{\alpha \downarrow 0} \frac{1}{\sin\alpha} \boldsymbol{d}(\alpha,\beta), \tag{17}$$

and

$$\boldsymbol{d}(\alpha, 2\pi - \alpha) = 2(1-\cos\alpha) \begin{bmatrix} \cos\alpha \\ -1 \end{bmatrix}. \tag{18}$$

Lemma 4: Let $0 \le \alpha < \beta < 2\pi$ and let $\boldsymbol{d}(\alpha,\beta)$ be defined as in (16). Then the trigonometric polynomial $\mathrm{Re}\ \boldsymbol{v}(\theta;1)^{\mathrm{H}}\boldsymbol{d}(\alpha,\beta)$ satisfies the following properties:

$$\begin{cases} \mathrm{Re}\ \boldsymbol{v}(\theta;1)^{\mathrm{H}}\boldsymbol{d}(\alpha,\beta) > 0 \ \text{ for all } \theta \in (\alpha,\beta), \\ \mathrm{Re}\ \boldsymbol{v}(\theta;1)^{\mathrm{H}}\boldsymbol{d}(\alpha,\beta) < 0 \ \text{ for all } \theta \in [0,2\pi) \setminus [\alpha,\beta]. \end{cases}$$

Finally, we also need the following well known representation result for trigonometric polynomials which are non-negative over the entire unit circle.

Proposition 2 (Riesz-Féjer) Let $\boldsymbol{p} \in \mathbb{R} \times \mathbb{C}^n$. Then

$$\mathrm{Re}\ \boldsymbol{v}(\theta;n)^{\mathrm{H}}\boldsymbol{p} \ge 0 \text{ for all } \theta \in [0,2\pi)$$

if and only if there exists $\boldsymbol{q} \in \mathbb{R} \times \mathbb{C}^n$ such that

$$\mathrm{Re}\ \boldsymbol{v}(\theta;n)^{\mathrm{H}}\boldsymbol{p} = \left|\boldsymbol{v}(\theta;n)^{\mathrm{H}}\boldsymbol{q}\right|^2.$$

We are now ready to establish the main result of this section.

Theorem 2: Let $\boldsymbol{p} \in \mathbb{R} \times \mathbb{C}^n$, $0 \le \alpha < \beta < 2\pi$, and let $\boldsymbol{d}(\alpha,\beta)$ be given by (16). Then

$$\mathrm{Re}\ \boldsymbol{v}(\theta;n)^{\mathrm{H}}\boldsymbol{p} \ge 0 \ \text{ for all } \ \theta \in [\alpha,\beta] \tag{19}$$

if and only if there exist $\boldsymbol{q} \in \mathbb{R} \times \mathbb{C}^n$ and $\boldsymbol{r} \in \mathbb{R} \times \mathbb{C}^{n-1}$ such that

$$\operatorname{Re} \boldsymbol{v}(\theta; n)^{\mathrm{H}} \boldsymbol{p} = \left| \boldsymbol{v}(\theta; n)^{\mathrm{H}} \boldsymbol{q} \right|^2 + \left(\operatorname{Re} \boldsymbol{v}(\theta; 1)^{\mathrm{H}} \boldsymbol{d}(\alpha, \beta) \right) \left| \boldsymbol{v}(\theta; n-1)^{\mathrm{H}} \boldsymbol{r} \right|^2. \tag{20}$$

Moreover,

$$\operatorname{Re} \boldsymbol{v}(\theta; n)^{\mathrm{H}} \boldsymbol{p} \geq 0 \quad \text{for all} \quad \theta \in [0, 2\pi) \setminus (\alpha, \beta) \tag{21}$$

if and only if there exist $\boldsymbol{q} \in \mathbb{R} \times \mathbb{C}^n$ and $\boldsymbol{r} \in \mathbb{R} \times \mathbb{C}^{n-1}$ such that

$$\operatorname{Re} \boldsymbol{v}(\theta; n)^{\mathrm{H}} \boldsymbol{p} = \left| \boldsymbol{v}(\theta; n)^{\mathrm{H}} \boldsymbol{q} \right|^2 - \left(\operatorname{Re} \boldsymbol{v}(\theta; 1)^{\mathrm{H}} \boldsymbol{d}(\alpha, \beta) \right) \left| \boldsymbol{v}(\theta; n-1)^{\mathrm{H}} \boldsymbol{r} \right|^2. \tag{22}$$

Proof. In light of Lemma 4, it is obvious that (20) implies (19), and similarly (22) implies (21). We now establish the converse relations. Fix some $\boldsymbol{p} \in \mathbb{R} \times \mathbb{C}^n$ such that (19) holds. We introduce a vector $\tilde{\boldsymbol{p}} \in \mathbb{R}^{2n+1}$ as follows:

$$\begin{cases} \tilde{p}_{2i} = \operatorname{Re} p_i, & \text{for } i = 0, 1, \ldots, n, \\ \tilde{p}_{2i-1} = \operatorname{Im} p_i, & \text{for } i = 1, 2, \ldots, n. \end{cases}$$

Using Theorem 1 and its notations, we have

$$\operatorname{Re} \boldsymbol{v}(\theta; n)^{\mathrm{H}} \boldsymbol{p} = \frac{\boldsymbol{u}(\eta^{-1}(\theta); 2n)^{\mathrm{T}} \tilde{\boldsymbol{p}}}{(1 + (\eta^{-1}(\theta))^2)^2} \quad \text{for all} \quad \theta \in (0, 2\pi). \tag{23}$$

Recall from Theorem 1 that $\eta(t) := \arg((t+\mathrm{j})^2/(1+t^2))$ is a bijection between $\mathbb{R}$ and $(0, 2\pi)$. For convenience, we let $\eta(\infty) := 0$ to obtain a bijection between $\mathbb{R} \cup \{\infty\}$ and $[0, 2\pi)$. Let $a := \eta^{-1}(\alpha)$ and $b := \eta^{-1}(\beta)$. Since η is a bijection between $\mathbb{R} \cup \{\infty\}$ and $[0, 2\pi)$ and η is a decreasing function, it follows that

$$\eta([b, \infty)) = [0, \beta], \quad [b, \infty) = \eta^{-1}([0, \beta]).$$

and for $\alpha > 0$ that

$$\eta([b, a]) = [\alpha, \beta], \quad [b, a] = \eta^{-1}([\alpha, \beta]).$$

Since (19) holds, it follows from (23) that $\boldsymbol{u}(t; 2n)^{\mathrm{T}} \tilde{\boldsymbol{p}} \geq 0$ for all $t \in [a, b]$. As a result, we may apply Proposition 1 to conclude that for given α and β there exist $\tilde{\boldsymbol{q}} \in \mathbb{R}^{n+1}$ and $\tilde{\boldsymbol{r}} \in \mathbb{R}^n$ such that

$$\boldsymbol{u}(t; 2n)^{\mathrm{T}} \tilde{\boldsymbol{p}} = \left(\boldsymbol{u}(t; n)^{\mathrm{T}} \tilde{\boldsymbol{q}} \right)^2 + (t - b)(a - t) \left(\boldsymbol{u}(t; n-1)^{\mathrm{T}} \tilde{\boldsymbol{r}} \right)^2,$$

if $\alpha > 0$, or

$$\boldsymbol{u}(t; 2n)^{\mathrm{T}} \tilde{\boldsymbol{p}} = \left(\boldsymbol{u}(t; n)^{\mathrm{T}} \tilde{\boldsymbol{q}} \right)^2 + (t - b) \left(\boldsymbol{u}(t; n-1)^{\mathrm{T}} \tilde{\boldsymbol{r}} \right)^2,$$

if $\alpha = 0$. Due to Theorem 1 and Proposition 2, there must exist a $\boldsymbol{q} \in \mathbb{R} \times \mathbb{C}^n$ and a $\hat{\boldsymbol{r}} \in \mathbb{R} \times \mathbb{C}^{n-1}$ such that

$$\frac{\left(\boldsymbol{u}(t; n)^{\mathrm{T}} \tilde{\boldsymbol{q}} \right)^2}{(1 + t^2)^n} = \left| \boldsymbol{v}(\eta(t); n)^{\mathrm{H}} \boldsymbol{q} \right|^2,$$

and

$$\frac{\left(\boldsymbol{u}(t;n-1)^{\mathrm{T}}\tilde{\boldsymbol{r}}\right)^2}{(1+t^2)^{n-1}} = \left|\boldsymbol{v}(\eta(t);n-1)^{\mathrm{H}}\hat{\boldsymbol{r}}\right|^2.$$

Furthermore, we know from Theorem 1 that for given α and β there must exist some $\boldsymbol{c} \in \mathbb{R}\times\mathbb{C}$ such that

$$\frac{(t-b)(a-t)}{1+t^2} = \mathrm{Re}\ \boldsymbol{v}(\eta(t);1)^{\mathrm{H}}\boldsymbol{c}, \tag{24}$$

if $\alpha > 0$, or

$$\frac{t-b}{1+t^2} = \mathrm{Re}\ \boldsymbol{v}(\eta(t);1)^{\mathrm{H}}\boldsymbol{c}, \tag{25}$$

if $\alpha = 0$. We have now shown that (19) implies the existence of vectors $\boldsymbol{q}$, $\hat{\boldsymbol{r}}$ and $\boldsymbol{c}$ such that

$$\mathrm{Re}\ \boldsymbol{v}(\theta;n)^{\mathrm{H}}\boldsymbol{p} = \left|\boldsymbol{v}(\theta;n)^{\mathrm{H}}\boldsymbol{q}\right|^2 + \left(\mathrm{Re}\ \boldsymbol{v}(\theta;1)^{\mathrm{H}}\boldsymbol{c}\right)\left|\boldsymbol{v}(\theta;n-1)^{\mathrm{H}}\hat{\boldsymbol{r}}\right|^2.$$

With an analogous argument, using Corollary 2, Theorem 1 and Proposition 2, we can show that if (21) holds, then

$$\mathrm{Re}\ \boldsymbol{v}(\theta;n)^{\mathrm{H}}\boldsymbol{p} = \left|\boldsymbol{v}(\theta;n)^{\mathrm{H}}\boldsymbol{q}\right|^2 - \left(\mathrm{Re}\ \boldsymbol{v}(\theta;1)^{\mathrm{H}}\boldsymbol{c}\right)\left|\boldsymbol{v}(\theta;n-1)^{\mathrm{H}}\hat{\boldsymbol{r}}\right|^2.$$

It remains to show that $\boldsymbol{c}$ is a positive multiple of $\boldsymbol{d}(\alpha,\beta)$.

Notice that

$$\begin{aligned}
\mathrm{Re}\ \boldsymbol{v}(\eta(t);1)^{\mathrm{H}}\boldsymbol{c} &= \mathrm{Re}\ \boldsymbol{c}^{\mathrm{H}}\boldsymbol{v}(\eta(t);1) = \mathrm{Re}\ (c_0 + \overline{c}_1 e^{\mathrm{j}\eta(t)}) \\
&= \mathrm{Re}\ (c_0 + \overline{c}_1(\mathrm{j}+t)^2/(1+t^2)) \\
&= \frac{1}{(1+t^2)}\left(c_0 - \mathrm{Re}\ c_1 + 2t\ \mathrm{Im}\ c_1 + (c_0 + \mathrm{Re}\ c_1)t^2\right).
\end{aligned}$$

Comparing this with (24), we obtain for $\alpha > 0$ that

$$\frac{(t-b)(a-t)}{1+t^2} = \frac{1}{(1+t^2)}\left(c_0 - \mathrm{Re}\ c_1 + 2t\ \mathrm{Im}\ c_1 + (c_0 + \mathrm{Re}\ c_1)t^2\right).$$

This implies that

$$c_0 = -\frac{1+ab}{2}, \qquad c_1 = \frac{ab-1+(a+b)\mathrm{j}}{2}.$$

For $\alpha = 0$, we have to obtain $\boldsymbol{c}$ from the equation

$$\frac{t-b}{1+t^2} = \frac{1}{(1+t^2)}\left(c_0 - \mathrm{Re}\ c_1 + 2t\ \mathrm{Im}\ c_1 + (c_0 + \mathrm{Re}\ c_1)t^2\right),$$

yielding $c_0 = -b/2$ and $c_1 = (b+\mathrm{j})/2$. It is easily verified that

$$\boldsymbol{d}(\alpha,\beta) = \begin{cases} 2(1-\cos\alpha)(1-\cos\beta)\boldsymbol{c} & \text{for } \alpha > 0 \\ 2(1-\cos\beta)\boldsymbol{c} & \text{for } \alpha = 0. \end{cases}$$

We complete the proof by setting $\boldsymbol{r} = 2(1-\cos\alpha)(1-\cos\beta)\hat{\boldsymbol{r}}$ for $\alpha > 0$, and $\boldsymbol{r} = 2(1-\cos\beta)\hat{\boldsymbol{r}}$ for $\alpha = 0$.

Q.E.D.

Theorem 2 provides a complete analytical characterization of the set, say Ω, of trigonometric polynomials which are non-negative over a segment of the unit circle. In particular, it shows that any trigonometric polynomial in Ω can be written as a (non-negatively) weighted sum of two squared trigonometric polynomials (see (20)–(22)). This result will be used in next section to develop a linear matrix inequality representation of the polynomials in Ω.

IV. Linear Matrix Inequality Formulation

In this section, we shall use a result of Nesterov [24] and Theorem 2 of Section III to develop a linear matrix inequality (LMI) representation for Ω, the set of trigonometric polynomials which are non-negative over a segment of the unit circle.

In reference [24], Nesterov showed how to obtain a linear matrix inequality representation for the cone of functions representable as a (weighted) sum of squares of functions in a given linear functional space V_n. In our case, the linear functional space V_n under consideration is the space of all trigonometric polynomials of degree at most n. Clearly, the components of $\boldsymbol{v}(\theta; n)$ form a basis of V_n. Below we paraphrase the representation result of Nesterov for our functional space V_n.

Proposition 3: Let $\Delta \subseteq [0, 2\pi)$ be a given subset. Let there be m given trigonometric polynomials which are non-negative over Δ:

$$\mathrm{Re}\ \boldsymbol{v}(\theta; n_k)^{\mathrm{H}} \boldsymbol{w}_k \geq 0 \quad \text{for all} \quad \theta \in \Delta,$$

where for each $k = 1, 2, \ldots, m$, $n_k \in \{0, 1, ..., n\}$ and $\boldsymbol{w}_k \in \mathbb{R} \times \mathbb{C}^{n_k}$. Let $\mathsf{L}_k(\cdot) : \mathbb{C}^{n+1} \mapsto \mathbb{C}^{(n+1)\times(n+1)}$ be a linear operator such that

$$\mathsf{L}_k\big(\boldsymbol{v}(\theta; n)\big) + \mathsf{L}_k\big(\boldsymbol{v}(\theta; n)\big)^{\mathrm{H}} = 2\big(\mathrm{Re}\ \boldsymbol{v}(\theta; n_k)^{\mathrm{H}} \boldsymbol{w}_k\big) \boldsymbol{v}(\theta; n - n_k) \boldsymbol{v}(\theta; n - n_k)^{\mathrm{H}}, \quad \forall \theta \in [0, 2\pi).$$

Let $\ell \geq 1$ and $N \geq n + 1$. Consider the cone

$$\begin{aligned} \mathcal{K} = \big\{ \boldsymbol{p} \in \mathbb{R} \times \mathbb{C}^n \mid \quad & \mathrm{Re}\ \boldsymbol{v}(\theta; n)^{\mathrm{H}} \boldsymbol{p} = \sum_{k=0}^{\ell} \big(\mathrm{Re}\ \boldsymbol{v}(\theta; n_k)^{\mathrm{H}} \boldsymbol{w}_k\big) \sum_{m=0}^{N} \big| \boldsymbol{v}(\theta; n - n_k)^{\mathrm{H}} \boldsymbol{q}_{m,k} \big|^2 \\ & \text{for some } \boldsymbol{q}_{m,k} \in \mathbb{R} \times \mathbb{C}^{n - n_k} \big\}. \end{aligned} \tag{26}$$

Then we have the following alternative LMI description of $\mathcal{K}$:

$$\mathcal{K} = \left\{ \boldsymbol{p} \in \mathbb{R} \times \mathbb{C}^n \mid \boldsymbol{p} + \xi \mathrm{j} \boldsymbol{e}_0 = \sum_{k=1}^{m} \mathsf{L}_k^*(\boldsymbol{X}_k), \quad \text{for some } \boldsymbol{X}_k \in \mathcal{H}_+^{(n+1-n_k)\times(n+1-n_k)},\ \xi \in \mathbb{R} \right\},$$

where $\boldsymbol{e}_0$ is the first column of the $(n+1) \times (n+1)$ identity matrix and $\mathsf{L}_k^* : \mathbb{C}^{(n+1)\times(n+1)} \mapsto \mathbb{C}^{n+1}$ is the adjoint linear operator of L_k.

Consider now the set of (the real part of) trigonometric polynomials of order n, i.e. functions $\operatorname{Re} \boldsymbol{v}(\theta;n)^{\mathrm{H}}\boldsymbol{p}$ in $\theta \in [0, 2\pi)$, with coefficients $\boldsymbol{p} \in \mathbb{R} \times \mathbb{C}^n$. Given $0 \leq \alpha < \beta < 2\pi$, we define the sets

$$\mathcal{K}(\alpha,\beta) := \{\boldsymbol{p} \in \mathbb{R} \times \mathbb{C}^n \mid \operatorname{Re} \boldsymbol{v}(\theta;n)^{\mathrm{H}}\boldsymbol{p} \geq 0 \text{ for all } \theta \in [\alpha,\beta]\}, \tag{27}$$

and

$$\bar{\mathcal{K}}(\alpha,\beta) := \{\boldsymbol{p} \in \mathbb{R} \times \mathbb{C}^n \mid \operatorname{Re} \boldsymbol{v}(\theta;n)^{\mathrm{H}}\boldsymbol{p} \geq 0 \text{ for all } \theta \in [0,2\pi) \setminus (\alpha,\beta)\}. \tag{28}$$

Thus, $\mathcal{K}(\alpha,\beta)$ and $\bar{\mathcal{K}}(\alpha,\beta)$ describe the sets of (the real parts of) trigonometric polynomials which are non-negative over a segment of the unit circle. We also let

$$\mathcal{K}(0,2\pi) := \{\boldsymbol{p} \in \mathbb{R} \times \mathbb{C}^n \mid \operatorname{Re} \boldsymbol{v}(\theta;n)^{\mathrm{H}}\boldsymbol{p} \geq 0 \text{ for all } \theta \in [0,2\pi)\}, \tag{29}$$

describe the trigonometric polynomials that are nonnegative on the entire unit circle. We may interpret $\mathcal{K}(\alpha,\beta)$ and $\bar{\mathcal{K}}(\alpha,\beta)$ as convex cones in $\mathbb{R}^{2n+1}$. Since (the real part of) a trigonometric polynomial is non-negative on a closed segment if and only if it is non-negative on the corresponding open segment, these cones are invariant to the opening or closure of either end of the given segment. This fact simplifies the application of the LMI descriptions of these cones which we now develop. By Theorem 2, these cones can be equivalently described as

$$\begin{aligned}\mathcal{K}(\alpha,\beta) = \big\{\boldsymbol{p} \in \mathbb{R} \times \mathbb{C}^n \;\big|\; &\operatorname{Re} \boldsymbol{v}(\theta;n)^{\mathrm{H}}\boldsymbol{p} = |\boldsymbol{v}(\theta;n)^{\mathrm{H}}\boldsymbol{q}|^2 + (\operatorname{Re} \boldsymbol{v}(\theta;1)^{\mathrm{H}}\boldsymbol{d}(\alpha,\beta))\; |\boldsymbol{v}(\theta;n-1)^{\mathrm{H}}\boldsymbol{r}|^2 \\ &\text{for some } \boldsymbol{q} \in \mathbb{R} \times \mathbb{C}^n \text{ and } \boldsymbol{r} \in \mathbb{R} \times \mathbb{C}^{n-1}\big\}\end{aligned} \tag{30}$$

and

$$\begin{aligned}\bar{\mathcal{K}}(\alpha,\beta) = \big\{\boldsymbol{p} \in \mathbb{R} \times \mathbb{C}^n \;\big|\; &\operatorname{Re} \boldsymbol{v}(\theta;n)^{\mathrm{H}}\boldsymbol{p} = |\boldsymbol{v}(\theta;n)^{\mathrm{H}}\boldsymbol{q}|^2 - (\operatorname{Re} \boldsymbol{v}(\theta;1)^{\mathrm{H}}\boldsymbol{d}(\alpha,\beta))\; |\boldsymbol{v}(\theta;n-1)^{\mathrm{H}}\boldsymbol{r}|^2 \\ &\text{for some } \boldsymbol{q} \in \mathbb{R} \times \mathbb{C}^n \text{ and } \boldsymbol{r} \in \mathbb{R} \times \mathbb{C}^{n-1}\big\}\end{aligned} \tag{31}$$

where $\boldsymbol{d}(\alpha,\beta)$ is given by (16). Notice that both $\mathcal{K}(\alpha,\beta)$ and $\bar{\mathcal{K}}(\alpha,\beta)$ are in the form of (26), since each element of $\mathcal{K}(\alpha,\beta)$ or $\bar{\mathcal{K}}(\alpha,\beta)$ can be written as a (non-negatively) weighted sum of squares. Therefore, Proposition 3 implies $\mathcal{K}(\alpha,\beta)$ and $\bar{\mathcal{K}}(\alpha,\beta)$ both possess an LMI description. To derive an explicit form of these LMI representations, we need to make precise the linear operators L_k. This is what we do next.

We define the unit lower triangular $(n+1) \times (n+1)$ Toeplitz matrices $\boldsymbol{T}_{0,n},\ \boldsymbol{T}_{1,n},\ \ldots,\ \boldsymbol{T}_{n,n}$ as

$$[\boldsymbol{T}_{k,n}]_{ij} = \begin{cases} 1, & \text{if } i = k + j, \\ 0, & \text{otherwise,} \end{cases} \qquad \text{with } i,j \in \{0,1,\ldots,n\}. \tag{32}$$

Thus, $\boldsymbol{T}_{0,n} = \boldsymbol{I}$ and $\langle \boldsymbol{T}_{k,n}, \boldsymbol{X} \rangle = \sum_{\ell=0}^{n-k} \boldsymbol{X}_{\ell+k,\ell}$, for all $\boldsymbol{X} \in \mathbb{C}^{(n+1)\times(n+1)}$. That is, $\langle \boldsymbol{T}_{k,n}, \boldsymbol{X} \rangle$ is the sum of the elements on the kth lower off-diagonal of $\boldsymbol{X}$. Let us define a linear operator $\mathsf{L} : \mathbb{C}^{n+1} \mapsto \mathbb{C}^{(n+1)\times(n+1)}$ as

$$\mathsf{L}(\boldsymbol{y}) = y_0 \boldsymbol{T}_{0,n} + 2\sum_{i=1}^{n} y_i \boldsymbol{T}_{i,n}. \tag{33}$$

It can be checked that $\mathsf{L}(\boldsymbol{y})$ is lower triangular and

$$\mathsf{L}\big(\boldsymbol{v}(\theta;n)\big)+\mathsf{L}\big(\boldsymbol{v}(\theta;n)\big)^{\mathrm{H}}=2\boldsymbol{v}(\theta;n)\boldsymbol{v}(\theta;n)^{\mathrm{H}},\quad \text{for all } \theta\in[0,2\pi). \tag{34}$$

To determine the adjoint operator L^*, we note that

$$\langle \mathsf{L}(\boldsymbol{y}),\boldsymbol{X}\rangle=\bar{y}_0\langle \boldsymbol{T}_{0,n},\boldsymbol{X}\rangle+2\sum_{i=1}^{n}\overline{y}_i\langle \boldsymbol{T}_{i,n},\boldsymbol{X}\rangle=\boldsymbol{y}^{\mathrm{H}}\mathsf{L}^*(\boldsymbol{X}),\quad \forall\ \boldsymbol{X}\in\mathbb{C}^{(n+1)\times(n+1)},$$

where the adjoint $\boldsymbol{q}=\mathsf{L}^*(\boldsymbol{X})\in\mathbb{C}^{n+1}$ is given by

$$q_0=\langle \boldsymbol{T}_{0,n},\boldsymbol{X}\rangle,\quad q_i=2\langle \boldsymbol{T}_{i,n},\boldsymbol{X}\rangle,\quad \text{for } i=1,2,\ldots,n. \tag{35}$$

In addition, we need to define a family of operators $\Lambda(\boldsymbol{y};\alpha,\beta):\mathbb{C}^{n+1}\mapsto\mathbb{C}^{(n+1)\times(n+1)}$ which are linear in $\boldsymbol{y}\in\mathbb{C}^{n+1}$ and parameterized by $\alpha,\beta\in[0,2\pi]$. Let $\boldsymbol{d}(\alpha,\beta)=[d_0(\alpha,\beta),d_1(\alpha,\beta)]^{\mathrm{T}}$ be given by (16). Then

$$\begin{aligned}\Lambda(\boldsymbol{y};\alpha,\beta) \quad &:= \quad d_0(\alpha,\beta)\Big(y_0\boldsymbol{T}_{0,n-1}+2\sum_{k=1}^{n-1}y_k\boldsymbol{T}_{k,n-1}\Big)\\ &\qquad +\overline{d_1(\alpha,\beta)}\Big(\sum_{k=1}^{n}y_k\boldsymbol{T}_{k-1,n-1}\Big)+d_1(\alpha,\beta)\Big(\sum_{k=0}^{n-2}y_k\boldsymbol{T}_{k+1,n-1}\Big).\end{aligned}$$

It can be checked that

$$\Lambda\big(\boldsymbol{v}(\theta,n)\big)+\Lambda\big(\boldsymbol{v}(\theta,n)\big)^{\mathrm{H}}=2\big(\mathrm{Re}\ \boldsymbol{v}(\theta;1)^{\mathrm{H}}\boldsymbol{d}(\alpha,\beta)\big)\ \boldsymbol{v}(\theta;n-1)\boldsymbol{v}(\theta;n-1)^{\mathrm{H}},\quad \forall\ \theta\in[0,2\pi).$$

To determine the adjoint operator of Λ, we fix any $\boldsymbol{y}\in\mathbb{C}^{n+1}$ and any $\boldsymbol{X}\in\mathbb{C}^{n\times n}$ and consider

$$\begin{aligned}\langle\Lambda(\boldsymbol{y};\alpha,\beta),\boldsymbol{X}\rangle \quad &= \quad d_0(\alpha,\beta)\Big(\overline{y}_0\langle \boldsymbol{T}_{0,n-1},\boldsymbol{X}\rangle+2\sum_{k=1}^{n-1}\overline{y}_k\langle \boldsymbol{T}_{k,n-1},\boldsymbol{X}\rangle\Big)\\ &\qquad +d_1(\alpha,\beta)\Big(\sum_{k=1}^{n}\overline{y}_k\langle \boldsymbol{T}_{k-1,n-1},\boldsymbol{X}\rangle\Big)+\overline{d_1(\alpha,\beta)}\Big(\sum_{k=0}^{n-2}\overline{y}_k\langle \boldsymbol{T}_{k+1,n-1},\boldsymbol{X}\rangle\Big)\\ &= \quad \boldsymbol{y}^{\mathrm{H}}\Lambda^*(\boldsymbol{X};\alpha,\beta).\end{aligned}$$

Thus, the adjoint $\boldsymbol{q}=\Lambda^*(\boldsymbol{X};\alpha,\beta)$ is given by

$$\begin{cases} q_0=d_0(\alpha,\beta)\langle \boldsymbol{T}_{0,n-1},\boldsymbol{X}\rangle+\overline{d_1(\alpha,\beta)}\langle \boldsymbol{T}_{1,n-1},\boldsymbol{X}\rangle,\\ q_k=2d_0(\alpha,\beta)\langle \boldsymbol{T}_{k,n-1},\boldsymbol{X}\rangle+d_1(\alpha,\beta)\langle \boldsymbol{T}_{k-1,n-1},\boldsymbol{X}\rangle+\overline{d_1(\alpha,\beta)}\langle \boldsymbol{T}_{k+1,n-1},\boldsymbol{X}\rangle,\\ \qquad\qquad\qquad\qquad\qquad\qquad\qquad\qquad \text{for}\quad k=1,2,...,n-2,\\ q_{n-1}=2d_0(\alpha,\beta)\langle \boldsymbol{T}_{n-1,n-1},\boldsymbol{X}\rangle+d_1(\alpha,\beta)\langle \boldsymbol{T}_{n-2,n-1},\boldsymbol{X}\rangle,\\ q_n=d_1(\alpha,\beta)\langle \boldsymbol{T}_{n-1,n-1},\boldsymbol{X}\rangle.\end{cases} \tag{36}$$

Combining this with (30), (31) and (35) and invoking Proposition 3, we obtain the following key result.

Theorem 3: Let $0 \le \alpha < \beta < 2\pi$. Suppose $\mathcal{K}(\alpha,\beta)$ and $\bar{\mathcal{K}}(\alpha,\beta)$ are given by (27) and (28). Let L^* and $\mathsf{\Lambda}^*$ be the adjoint operators defined by (35) and (36). Then, the cones $\mathcal{K}(\alpha,\beta)$ and $\bar{\mathcal{K}}(\alpha,\beta)$ admit the following LMI description:

$$\begin{aligned}\mathcal{K}(\alpha,\beta) = \big\{\boldsymbol{p} \,\big|\quad & \boldsymbol{p} + \xi \mathrm{j}\boldsymbol{e}_0 = \mathsf{L}^*(\boldsymbol{X}) + \mathsf{\Lambda}^*(\boldsymbol{Z};\alpha,\beta) \\ & \text{for some } \boldsymbol{X} \in \mathcal{H}_+^{(n+1)\times(n+1)},\ \boldsymbol{Z} \in \mathcal{H}_+^{n\times n},\ \xi \in \mathbb{R}\big\},\end{aligned} \tag{37}$$

and

$$\begin{aligned}\bar{\mathcal{K}}(\alpha,\beta) = \big\{\boldsymbol{p} \,\big|\quad & \boldsymbol{p} + \xi \mathrm{j}\boldsymbol{e}_0 = \mathsf{L}^*(\boldsymbol{X}) - \mathsf{\Lambda}^*(\boldsymbol{Z};\alpha,\beta) \\ & \text{for some } \boldsymbol{X} \in \mathcal{H}_+^{(n+1)\times(n+1)},\ \boldsymbol{Z} \in \mathcal{H}_+^{n\times n},\ \xi \in \mathbb{R}\big\}.\end{aligned} \tag{38}$$

Moreover,

$$\mathcal{K}(0,2\pi) = \big\{\mathsf{L}^*(\boldsymbol{X}) \,\big|\boldsymbol{X} \in \mathcal{H}_+^{(n+1)\times(n+1)}\big\}. \tag{39}$$

Theorem 3 provides an equivalent LMI description for a trigonometric polynomial which is non-negative over a given segment $[\alpha,\beta]$ (or its complement) of the unit circle. (Observe that $\mathcal{K}(\alpha,2\pi) = \bar{\mathcal{K}}(0,\alpha)$.) As mentioned in Section I, this LMI formulation is of practical interest because it generates a precise finite representation of the spectral mask constraints often encountered in the design of digital filters. Furthermore, the LMI formulation of the mask results in filter design problems that can be efficiently solved via well-established interior point methods [25]. We will give some detailed examples in Section V.

Equation (39) is a new formulation of the Positive Real Lemma [16, 17] (and the closely related Kalman-Yakubovich-Popov [KYP] Lemma) for FIR systems (see also [24] and Section 3.2 in [26]). The new formulation is the dual of the standard formulation, and states that for r_m, $-M+1 \le m \le M-1$, with $r_{-m} = \bar{r}_m$, $R(e^{\mathrm{j}\theta}) \ge 0$ for all $\theta \in [0,2\pi)$ if and only if there exists an $\boldsymbol{X} \in \mathcal{H}_+^{M\times M}$ such that $\mathrm{tr}(\boldsymbol{X}) = r_0$ and $\sum_{\ell=0}^{M-1-m} [\boldsymbol{X}]_{\ell+m,\ell} = r_m$, for $1 \le m \le M-1$. Thus, Theorem 3 can be seen as an extension of Positive Real Lemma for FIR systems.

Now let us consider the special case of real trigonometric polynomials of the form $\sum_{k=0}^{n} p_k \cos(k\theta)$ with coefficients $\boldsymbol{p} \in \mathbb{R}^{n+1}$, and segments of the form $[\alpha, 2\pi-\alpha]$. Since $\cos(k\theta)$ and the segment are symmetric with respect to $\theta = \pi$, we need only consider the sub-segment $[\alpha,\pi]$ and the LMI descriptions in Theorem 3 can be simplified to

$$\begin{aligned}\mathcal{K}_{\mathrm{real}}(\alpha) &= \left\{\boldsymbol{p} \in \mathbb{R}^{n+1} \,\middle|\, \sum_{k=0}^{n} p_k \cos(k\theta) \ge 0, \quad \text{for all } \theta \in [\alpha,\pi]\right\} \\ &= \left\{\boldsymbol{p} \,\middle|\, \boldsymbol{p} = \mathsf{L}^*(\boldsymbol{X}) + \mathsf{\Lambda}^*(\boldsymbol{Z};\alpha,2\pi-\alpha),\ \text{ for some } \boldsymbol{X} \in \mathcal{S}_+^{(n+1)\times(n+1)},\ \boldsymbol{Z} \in \mathcal{S}_+^{n\times n}\right\},\end{aligned} \tag{40}$$

(for non-negativity on $[\alpha, \pi]$) and

$$\begin{aligned}\bar{\mathcal{K}}_{\text{real}}(\alpha) &= \left\{ \boldsymbol{p} \in \mathbb{R}^{n+1} \;\middle|\; \sum_{k=0}^{n} p_k \cos(k\theta) \geq 0, \quad \text{for all } \theta \in [0, \alpha] \right\} \\ &= \left\{ \boldsymbol{p} \;\middle|\; \boldsymbol{p} = \mathsf{L}^*(\boldsymbol{X}) - \mathsf{\Lambda}^*(\boldsymbol{Z}; \alpha, 2\pi - \alpha), \;\text{ for some } \boldsymbol{X} \in \mathcal{S}_+^{(n+1)\times(n+1)},\, \boldsymbol{Z} \in \mathcal{S}_+^{n\times n} \right\}, \qquad (41)\end{aligned}$$

(for non-negativity on $[0, \alpha]$), where $\mathsf{\Lambda}^*(\boldsymbol{Z}; \alpha, 2\pi - \alpha)$ is given by (36) with $d_0(\alpha, 2\pi - \alpha)$ and $d_1(\alpha, 2\pi - \alpha)$ simplified to be [see (18)]

$$d_0(\alpha, 2\pi - \alpha) = 2\cos\alpha(1 - \cos\alpha) \quad \text{and} \quad d_1(\alpha, 2\pi - \alpha) = -2(1 - \cos\alpha). \qquad (42)$$

Notice that $\boldsymbol{X}$ and $\boldsymbol{Z}$ in (40) [and (41)] are real symmetric, rather than complex Hermitian. To see why we can restrict to real symmetric matrices, consider a Hermitian positive semidefinite matrix $\boldsymbol{X} = (\text{Re } \boldsymbol{X}) + \text{j}(\text{Im } \boldsymbol{X})$ given in the representation (37). Since $\boldsymbol{X} \succeq 0$, for real $\boldsymbol{q} \in \mathbb{R}^n$ we have that

$$0 \leq \boldsymbol{q}^{\mathrm{T}} \boldsymbol{X} \boldsymbol{q} = \boldsymbol{q}^{\mathrm{T}} (\text{Re } \boldsymbol{X}) \boldsymbol{q} + \text{j} \boldsymbol{q}^{\mathrm{T}} (\text{Im } \boldsymbol{X}) \boldsymbol{q} = \boldsymbol{q}^{\mathrm{T}} (\text{Re } \boldsymbol{X}) \boldsymbol{q}.$$

Hence, Re $\boldsymbol{X} \in \mathcal{S}_+^{n\times n}$. Moreover, Re $\langle \boldsymbol{T}_{i,n}, \boldsymbol{X} \rangle = \langle \boldsymbol{T}_{i,n}, \text{Re } \boldsymbol{X} \rangle$. Thus, if the imaginary parts of the coefficients p_i are restricted to zero, then since d_0 and d_1 in (42) are real, we can replace $\boldsymbol{X}$ and $\boldsymbol{Z}$ [obtained from (37)] by Re $\boldsymbol{X}$ and Re $\boldsymbol{Z}$, with both Re $\boldsymbol{X}$ and Re $\boldsymbol{Z}$ still being positive semidefinite.

V. Applications

We now show how the results of Section IV can be applied to the design of FIR filters and to data-independent narrowband beamformers.

A. FIR Filter Design

In optimization-based designs of (real-valued) FIR filters, one often encounters a (relative) spectral mask constraint of the form

$$\zeta \breve{L}(e^{\text{j}\theta}) \leq \left|G(e^{\text{j}\theta})\right| \leq \zeta \breve{U}(e^{\text{j}\theta}) \qquad \text{for all } \theta \in [0, \pi], \qquad (43)$$

where $\zeta > 0$, and a normalization constraint either on the filter coefficients or on ζ. [We have used the 'breve' notation to distinguish (43) from (1).] As discussed in the introduction, the mask constraint can be made convex by constraining $G(e^{\text{j}\theta})$ to have 'linear phase', or by reformulating the constraint in terms of the autocorrelation sequence $r_m = \sum_k g_k g_{k-m}$ as $\zeta^2 \breve{L}(e^{\text{j}\theta})^2 \leq R(e^{\text{j}\theta}) \leq \zeta^2 \breve{U}(e^{\text{j}\theta})^2$. In both these cases, we can exploit the results of Section IV to precisely transform the piecewise constant and piecewise trigonometric polynomial portions of the mask into pairs of LMIs. The first step is to write $G(e^{\text{j}\theta})$ or $R(e^{\text{j}\theta})$ in the form

$\mathrm{Re}\,\boldsymbol{v}(\theta;\cdot)^{\mathrm{H}}\boldsymbol{p}$. To do so, we define $\boldsymbol{M} \in \mathbb{R}^{(2M-1)\times M}$ and $\tilde{\boldsymbol{I}} \in \mathbb{R}^{M\times M}$ such that

$$\boldsymbol{M} := \begin{bmatrix} \boldsymbol{0} & \boldsymbol{J} \\ 1 & \boldsymbol{0} \\ \boldsymbol{0} & \boldsymbol{I} \end{bmatrix} \qquad \text{and} \qquad \tilde{\boldsymbol{I}} := \begin{bmatrix} 1 & \boldsymbol{0} \\ \boldsymbol{0} & 2\boldsymbol{I} \end{bmatrix}, \tag{44}$$

where $\boldsymbol{I}$ is the $(M-1)\times(M-1)$ identity matrix and $\boldsymbol{J}$ is the $(M-1)\times(M-1)$ matrix with ones on the anti-diagonal and zeros elsewhere. For a filter of length M, if we define $\tilde{\boldsymbol{r}} \in \mathbb{R}^M$ such that $[\tilde{\boldsymbol{r}}]_m = r_m$, $0 \le m \le M-1$, then

$$R(e^{\mathrm{j}\theta}) = e^{\mathrm{j}(M-1)\theta}\boldsymbol{v}\big(\theta; 2(M-1)\big)^{\mathrm{H}}\boldsymbol{M}\tilde{\boldsymbol{r}} = \mathrm{Re}\,\boldsymbol{v}(\theta; M-1)^{\mathrm{H}}\tilde{\boldsymbol{I}}\tilde{\boldsymbol{r}}.$$

Similarly, for a filter of odd length $2M-1$ which is symmetric and centered at the origin, if we define $\tilde{\boldsymbol{g}} \in \mathbb{R}^M$ such that $[\tilde{\boldsymbol{g}}]_k = g_k$, $0 \le k \le M-1$ then, $G(e^{\mathrm{j}\theta}) = \mathrm{Re}\,\boldsymbol{v}(\theta; M-1)^{\mathrm{H}}\tilde{\boldsymbol{I}}\tilde{\boldsymbol{g}}$. The frequency response of other linear phase filters can be written in related ways, but for brevity we will consider only the odd-length symmetric case.

To further simplify our exposition, we will first consider the design of a simple low-pass filter with a piecewise constant mask. A natural extension to a piecewise trigonometric polynomial mask is provided later in this section, and extensions to band-pass and multi-band filters are implicit in the design in Section V–B. The simple piecewise constant low-pass spectral mask can be written in the form of (43), where

$$\breve{L}(e^{\mathrm{j}\theta}) = \begin{cases} \breve{L}_p & 0 \le \theta \le 2\pi f_p \\ \breve{L}_t & 2\pi f_p < \theta \le 2\pi f_s \\ \breve{L}_s & 2\pi f_s < \theta \le \pi \end{cases} \qquad \text{and} \qquad \breve{U}(e^{\mathrm{j}\theta}) = \begin{cases} \breve{U}_p & 0 \le \theta < 2\pi f_s \\ \breve{U}_s & 2\pi f_s \le \theta \le \pi, \end{cases} \tag{45}$$

with f_p and f_s denoting the normalized frequencies of the pass-band and stop-band edges, respectively, $0 \le f_p < f_s \le 1/2$, and $0 < \breve{U}_s \le \breve{U}_p$, $0 \le \breve{L}_p < \breve{U}_p$ and $\breve{L}_s \le \breve{L}_p$. In the case of linear phase filters we set $\breve{L}_t = -\breve{U}_p$ and $\breve{L}_s = -\breve{U}_s$, whereas for autocorrelation designs we set $\breve{L}_t = \breve{L}_s = 0$. By observing the common form of $G(e^{\mathrm{j}\theta})$ and $R(e^{\mathrm{j}\theta})$ above, and that $\breve{L}_t \le \breve{L}_s \le \breve{L}_p$ and $\breve{U}_s \le \breve{U}_p$, the spectral mask constraint can be re-written in a generic form as

$$\begin{cases} \tilde{\boldsymbol{I}}\tilde{\boldsymbol{x}} - \zeta^q \breve{L}_p^q \boldsymbol{e}_0 \in \bar{\mathcal{K}}_{\mathrm{real}}(2\pi f_p) \\ \tilde{\boldsymbol{I}}\tilde{\boldsymbol{x}} - \zeta^q \breve{L}_t^q \boldsymbol{e}_0 \in \mathcal{K}_{\mathrm{real}}(0) \\ \tilde{\boldsymbol{I}}\tilde{\boldsymbol{x}} - \zeta^q \breve{L}_s^q \boldsymbol{e}_0 \in \mathcal{K}_{\mathrm{real}}(2\pi f_s) \end{cases} \qquad \text{and} \qquad \begin{cases} \zeta^q \breve{U}_p^q \boldsymbol{e}_0 - \tilde{\boldsymbol{I}}\tilde{\boldsymbol{x}} \in \mathcal{K}_{\mathrm{real}}(0) \\ \zeta^q \breve{U}_s^q \boldsymbol{e}_0 - \tilde{\boldsymbol{I}}\tilde{\boldsymbol{x}} \in \mathcal{K}_{\mathrm{real}}(2\pi f_s), \end{cases} \tag{46}$$

where $q = 1$ and $\tilde{\boldsymbol{x}} = \tilde{\boldsymbol{g}}$ when we design an odd-length symmetric filter, and $q = 2$ and $\tilde{\boldsymbol{x}} = \tilde{\boldsymbol{r}}$ for autocorrelation designs. For autocorrelation designs, $\breve{L}_t = \breve{L}_s = 0$ and hence the constraint $\tilde{\boldsymbol{I}}\tilde{\boldsymbol{x}} - \zeta^q \breve{L}_s^q \boldsymbol{e}_0 \in \mathcal{K}_{\mathrm{real}}(2\pi f_s)$ is redundant.

The constraints in (46) define the set of feasible filters. The question that remains is which of these filters is the 'best'. A large class of filter design objectives can be cast as the minimization of a convex quadratic function of the parameters. This class includes the weighted least-squares approximation of some desired magnitude response [3, 4, 9]. Filter design problems in this class take the following form: Given a positive semidefinite matrix $\boldsymbol{Q}$, a vector $\boldsymbol{l}$ and an integer $q \in \{1, 2\}$, find $\tilde{\boldsymbol{x}}$ achieving

$$\min_{\tilde{\boldsymbol{x}}} \tilde{\boldsymbol{x}}^{\mathrm{T}} \boldsymbol{Q} \tilde{\boldsymbol{x}} - 2\boldsymbol{l}^{\mathrm{T}} \tilde{\boldsymbol{x}} \tag{47}$$

subject to (46) and a linear normalization constraint on either $\tilde{\boldsymbol{x}}$ or ζ, or show that none exist. This generic design problem can be solved by solving the following convex optimization problem:

Problem 1: Given q from (46), and given $\boldsymbol{Q} = \boldsymbol{L}\boldsymbol{L}^{\mathrm{T}}$, $\boldsymbol{l}$, f_p, f_s, $\breve{L}_p$, $\breve{L}_t$ $\breve{L}_s$, $\breve{U}_p$, $\breve{U}_s$, and M, find $\tilde{\boldsymbol{x}} \in \mathbb{R}^M$ achieving min $\Gamma - 2\boldsymbol{l}^{\mathrm{T}} \tilde{\boldsymbol{x}}$ over $\tilde{\boldsymbol{x}}$, $\zeta > 0$, $\boldsymbol{X}^{(pu)}, \boldsymbol{X}^{(pl)}, \boldsymbol{X}^{(t)}, \boldsymbol{X}^{(su)} \in \mathcal{S}_+^{M \times M}$, $\boldsymbol{Z}^{(pl)}, \boldsymbol{Z}^{(su)} \in \mathcal{S}_+^{(M-1)\times(M-1)}$, and, if $q = 1$, $\boldsymbol{X}^{(s\ell)} \in \mathcal{S}_+^{M \times M}$ and $\boldsymbol{Z}^{(s\ell)} \in \mathcal{S}_+^{M-1 \times M-1}$, subject to $\|\boldsymbol{L}^{\mathrm{T}} \tilde{\boldsymbol{x}}\|_2^2 \leq \Gamma$,

$$\tilde{\boldsymbol{I}} \tilde{\boldsymbol{x}} - \zeta^q \breve{L}_p^q \boldsymbol{e}_0 = \mathsf{L}^*(\boldsymbol{X}^{(pl)}) - \mathsf{\Lambda}^*\big(\boldsymbol{Z}^{(pl)}; 2\pi f_p, 2\pi(1 - f_p)\big), \tag{48}$$

$$\tilde{\boldsymbol{I}} \tilde{\boldsymbol{x}} - \zeta^q \breve{L}_t^q \boldsymbol{e}_0 = \mathsf{L}^*(\boldsymbol{X}^{(t)}), \tag{49}$$

$$\zeta^q \breve{U}_p^q \boldsymbol{e}_0 - \tilde{\boldsymbol{I}} \tilde{\boldsymbol{x}} = \mathsf{L}^*(\boldsymbol{X}^{(pu)}), \tag{50}$$

$$\zeta^q \breve{U}_s^q \boldsymbol{e}_0 - \tilde{\boldsymbol{I}} \tilde{\boldsymbol{x}} = \mathsf{L}^*(\boldsymbol{X}^{(su)}) + \mathsf{\Lambda}^*\big(\boldsymbol{Z}^{(su)}; 2\pi f_s, 2\pi(1 - f_s)\big), \tag{51}$$

and, if $q = 1$,

$$\tilde{\boldsymbol{I}} \tilde{\boldsymbol{x}} - \zeta^q \breve{L}_s^q \boldsymbol{e}_0 = \mathsf{L}^*(\boldsymbol{X}^{(s\ell)}) + \mathsf{\Lambda}^*\big(\boldsymbol{Z}^{(sl)}; 2\pi f_s, 2\pi(1 - f_s)\big), \tag{52}$$

and one of the normalizations $\zeta = 1$ or $\boldsymbol{c}^{\mathrm{T}} \tilde{\boldsymbol{x}} = 1$, for a given vector $\boldsymbol{c}$, or show that none exist.

In Problem 1, Eqs (48), (49) and (52) enforce the lower bound constraint of the spectral mask, and Eqs (50) and (51) enforce the upper bound constraint. Problem 1 consists of a linear objective, linear equality constraints [(48)–(51), and (52) where applicable], a linear inequality constraint on ζ, positive semidefiniteness constraints on the various $\boldsymbol{X}$ and $\boldsymbol{Z}$ matrices, and the constraint $\|\boldsymbol{L}^{\mathrm{T}} \tilde{\boldsymbol{x}}\|_2^2 \leq \Gamma$. The set of vectors $[\Gamma, (\boldsymbol{L}^{\mathrm{T}} \tilde{\boldsymbol{x}})^{\mathrm{T}}]^{\mathrm{T}} \in \mathbb{R}^{M+1}$ which satisfy this last constraint can be transformed to the intersection of a 'rotated' second-order cone in $\mathbb{R}^{M+2}$ and a hyperplane (e.g., [26]). Hence, Problem 1 is a convex symmetric cone programme [27, 28], which can be efficiently solved using well established interior point methods [29]. Furthermore, infeasibility can be reliably detected. If $\tilde{\boldsymbol{x}}$ represents the autocorrelation sequence of the filter, then an optimal filter can be obtained from the solution of Problem 1 by spectral factorization [9, 11].

We now demonstrate the flexibility of this design method by solving a number of filter design problems using small variations on Problem 1.

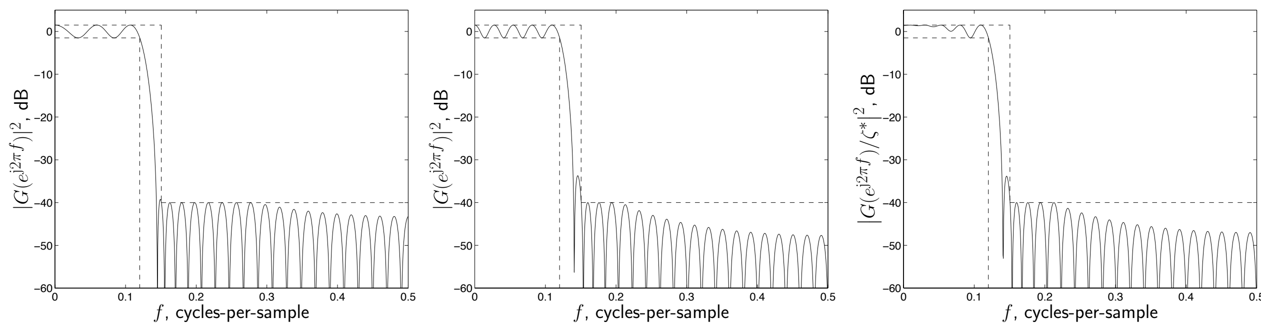

(a) Linear-phase filter minimizing stop-band energy.

(b) Nonlinear-phase filter minimizing stop-band energy.

(c) Nonlinear-phase filter minimizing proportion of energy in stop band.

Fig. 1. Power spectra of length 49 filters from Example 1, along with the corresponding mask. In (c), ζ^* is the optimal value of ζ from Problem 1.

Example 1: Consider the design of a length 49 FIR filter which has the minimal 'stop-band energy', $E_s = (1/\pi)\int_{2\pi f_c}^{\pi} |G(e^{\mathrm{j}\theta})|^2\, d\theta$, subject to the spectral mask in (45), with $f_p = 590/4915.2$, $f_s = 740/4915.2$, $\breve{L}_p^2 = 10^{-0.15}$, $\breve{U}_p^2 = 10^{0.15}$, $\breve{U}_s^2 = 10^{-4}$; i.e., $f_p \approx 0.12$, $f_s \approx 0.15$, ± 1.5 dB pass-band ripple, and 40 dB stop-band suppression. (The choice of this particular mask is explained in Example 3.) For an odd-length symmetric filter, $E_s = \tilde{\boldsymbol{g}}^{\mathrm{T}}\boldsymbol{Q}\tilde{\boldsymbol{g}}$, where $\boldsymbol{Q} = \tilde{\boldsymbol{I}}\check{\boldsymbol{Q}}\tilde{\boldsymbol{I}}$, $[\check{\boldsymbol{Q}}]_{ij} = 2\big(\mathrm{sinc}(i+j) + \mathrm{sinc}(i-j)\big) - 4f_c\big(\mathrm{sinc}(2f_c(i+j)) + \mathrm{sinc}(2f_c(i-j))\big)$, for $0 \le i, j \le M-1$, and $\mathrm{sinc}(x) = \sin(\pi x)/(\pi x)$ for $x \neq 0$ and 1 for $x = 0$. For a general filter, $E_s = \tilde{\boldsymbol{l}}^{\mathrm{T}}\tilde{\boldsymbol{r}}$, where $\tilde{l}_0 = 1/2 - f_c$ and $\tilde{l}_m = -2f_c\,\mathrm{sinc}(2f_c m)$, for $1 \le m \le M-1$. Therefore, optimal filters can be designed using Problem 1 with the normalization constraint $\zeta = 1$. For $f_c = (f_p + f_s)/2$, the power spectrum of the optimal linear phase filter is shown in Figure 1(a) and that of an optimal nonlinear phase filter is shown in Figure 1(b). Each design problem was solved using a MATLAB-based general-purpose symmetric cone programme solver called `SeDuMi` [26]. The linear-phase case was solved in 3.5 seconds on a 400 MHz PENTIUM II workstation, while the nonlinear phase case required 24 seconds. The sharper cut off and improved high-frequency decay of the nonlinear phase filter are clear from these figures. Although these filters minimize the stop-band energy, they do not minimize the proportion of the total energy of the filter in the stop band. A nonlinear phase filter which does so can be found by removing the constraint $\zeta = 1$ from Problem 1 (and hence allowing the mask to 'float'), and replacing it with $r_0 = 1$. The resulting optimal autocorrelation was obtained in 25 seconds and the power spectrum of an optimal filter is shown in Figure 1(c). Observe that the flatter passband response in this case is achieved without greatly affecting the stop-band decay. $\square$

In some applications one may wish to enforce a spectral mask constraint which is not piecewise constant.

For example, one may wish to have a 'roll-off' zone which provides a more gradual transition between the pass-band and stop-band in Figure 1. (See Figure 2 for an example.) We will now demonstrate how the large and diverse class of piecewise trigonometric polynomial masks can be precisely enforced using Theorem 3. For simplicity we will restrict our attention to the case of enforcing a roll-off constraint on a low-pass filter, but the techniques can be easily generalized. Let f_r denote the frequency at the 'left edge' of the roll-off portion of the mask, and let f_s denote the frequency at the left edge of the subsequent constant portion. Let the portion of $\breve{U}(e^{\mathrm{j}\theta})^q$ in the roll-off region be described by the real part of a trigonometric polynomial; i.e., let $\breve{U}(e^{\mathrm{j}\theta})^q = \mathrm{Re}\ B_q(e^{\mathrm{j}\theta})$ for $\theta \in [2\pi f_r, 2\pi f_s]$, where $B_q(e^{\mathrm{j}\theta}) = \sum_{k=0}^{M_{B_q}-1} b_{q,k} e^{-\mathrm{j}\theta k}$. Then this portion of the mask can be described in the notation of Section IV and Problem 1 by

$$\zeta^q \boldsymbol{b}_q - \tilde{\boldsymbol{I}}\tilde{\boldsymbol{x}} \in \mathcal{K}(2\pi f_r, 2\pi f_s), \tag{53}$$

where either $\boldsymbol{b}_q$ or $\tilde{\boldsymbol{x}}$ is to be padded with zeros so that they are both of dimension $\tilde{M} = \max\{M_{B_q}, M\}$. For linear phase filters, the roll-off must also be incorporated into the lower mask, $\breve{L}(e^{\mathrm{j}\theta})$, because $G(e^{\mathrm{j}\theta})$ is not constrained to be non-negative; i.e., $\breve{L}(e^{\mathrm{j}\theta}) = -\mathrm{Re}\ B_1(e^{\mathrm{j}\theta})$ for $\theta \in [2\pi f_r, 2\pi f_s]$. Hence, for the linear phase case we require (53) and

$$\tilde{\boldsymbol{I}}\tilde{\boldsymbol{x}} + \zeta \boldsymbol{b}_1 \in \mathcal{K}(2\pi f_r, 2\pi f_s). \tag{54}$$

For this roll-off example, the complete spectral mask is described by (46), (53) and (54), with (54) being redundant in the case of autocorrelation design. Therefore, the design of nonlinear phase filters which minimize the objective in (47) subject to the new mask can be achieved by adding two variables, $\boldsymbol{X}^{(ro)} \in \mathcal{H}_+^{\tilde{M}\times\tilde{M}}$ and $\boldsymbol{Z}^{(ro)} \in \mathcal{H}_+^{(\tilde{M}-1)\times(\tilde{M}-1)}$, to Problem 1, along with the additional constraint

$$\zeta^q \boldsymbol{b}_q - \tilde{\boldsymbol{I}}\tilde{\boldsymbol{x}} - \xi^{(ro)}\mathrm{j}\boldsymbol{e}_0 = \mathsf{L}^*(\boldsymbol{X}^{(ro)}) + \Lambda^*\big(\boldsymbol{Z}^{(ro)}; 2\pi f_r, 2\pi f_s\big), \tag{55}$$

where $\xi^{(ro)} \in \mathbb{R}$ is unconstrained. (Note that in Problem 1, $\tilde{\boldsymbol{x}}$ is already constrained to be real.) For linear phase filters, we require two more variables, $\boldsymbol{X}^{(rol)} \in \mathcal{H}_+^{\tilde{M}\times\tilde{M}}$ and $\boldsymbol{Z}^{(rol)} \in \mathcal{H}_+^{(\tilde{M}-1)\times(\tilde{M}-1)}$, and the additional constraint

$$\tilde{\boldsymbol{I}}\tilde{\boldsymbol{x}} + \zeta \boldsymbol{b}_1 - \xi^{(rol)}\mathrm{j}\boldsymbol{e}_0 = \mathsf{L}^*(\boldsymbol{X}^{(rol)}) + \Lambda^*\big(\boldsymbol{Z}^{(rol)}; 2\pi f_r, 2\pi f_s\big), \tag{56}$$

where $\xi^{(rol)} \in \mathbb{R}$ is unconstrained. In the following example, we re-visit the designs in Example 1 with a new mask which contains a roll-off section.

Example 2: Consider the mask from Example 1 and introduce a 'tighter' stop-band constraint consisting of a first-order trigonometric polynomial roll-off on the magnitude spectrum between $f_r = 740/4915.2$ and $f_s = 0.25$ and a constant bound on the magnitude for $0.25 \leq f \leq 0.5$. More specifically, in the roll-off region $\omega \in [2\pi f_r, 2\pi f_s]$, we enforce $|G(e^{\mathrm{j}\omega})| \leq \zeta B_1(e^{\mathrm{j}\omega})$, where the first-order trigonometric polynomial $B_1(e^{\mathrm{j}\omega})$ has real coefficients $b_{1,0}$ and $b_{1,1}$ chosen such that $B_1(e^{\mathrm{j}2\pi f_r}) = 10^{-2}$ and $B_1(e^{\mathrm{j}2\pi f_s}) = 10^{-2.5}$, and in the constant portion of the stop-band, $\omega \in [2\pi f_s, \pi]$, we enforce $|G(e^{\mathrm{j}\omega})| \leq \zeta 10^{-2.5}$. That is, the roll-off 'starts'

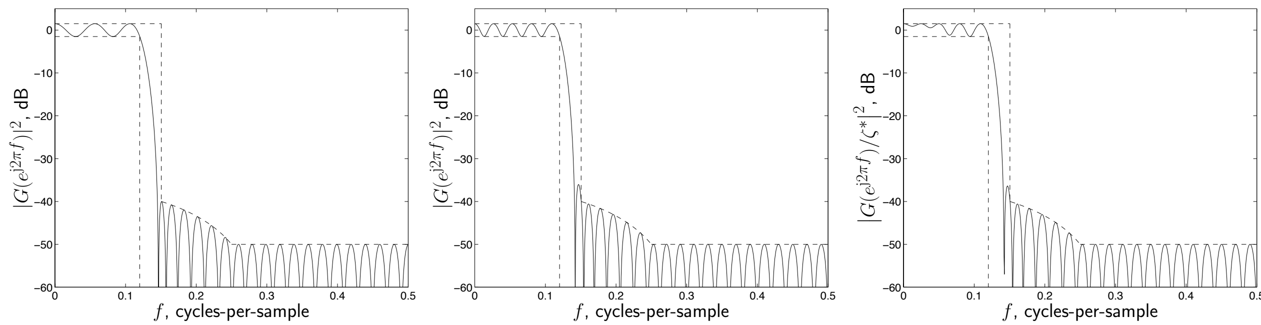

(a) Linear-phase filter minimizing stop-band energy.

(b) Nonlinear-phase filter minimizing stop-band energy.

(c) Nonlinear-phase filter minimizing proportion of energy in stop band.

Fig. 2. Power spectra of length 49 filters from Example 2, along with the corresponding mask. In (c), ζ^* is the optimal value of ζ.

at $f_r \approx 0.15$ with a suppression level of 40 dB and rolls off to a suppression level of 50 dB at $f_s = 0.25$, from which point the required suppression level remains 50 dB (see Figure 2). Note that since $R(e^{j\omega}) = |G(e^{j\omega})|^2$, $|G(e^{j\omega})| \leq \zeta B_1(e^{j\omega})$ for $\omega \in [2\pi f_r, 2\pi f_s]$ can be imposed directly on the power spectrum by enforcing $R(e^{j\omega}) \leq \zeta^2 B_2(e^{j\omega})$ for $\omega \in [2\pi f_r, 2\pi f_s]$, where $B_2(e^{j\omega})$ is a second-order trigonometric polynomial with coefficients $b_{2,0} = b_{1,0}^2 + b_{1,1}^2/2$, $b_{2,1} = 2b_{1,0}b_{1,1}$, and $b_{2,2} = b_{1,1}^2/2$. The power spectra of the length 49 linear and nonlinear phase filters which minimize the stop-band energy with $f_c = (f_p + f_r)/2$, subject to the spectral mask are shown in Figures 2(a) and (b), and that of the nonlinear phase filter which minimizes the proportion of the total energy of the filter in the stop-band is shown in Figure 2(c). (The optimal designs were obtained in 14, 95 and 99 seconds, respectively, using the set-up described in Example 1.) Note that these filters have similar pass-band characteristics to the corresponding filters in Example 1, but that the stop-band characteristics are substantially altered by the new mask. □

In the transmission of digital data by pulse amplitude modulation (PAM), we often encounter design specifications in terms of a spectral mask of the form in Figure 1. In fact, the mask in Figure 1 is that specified for the 'chip' waveform in the IS95 digital cellular communication standard [30]. A simplified block diagram of a PAM scheme is shown in Figure 3. The transmitted power is normalized to unity; i.e., $r_0 = 1$. In order to control the intersymbol interference (ISI) in a distortionless channel we can enforce the constraint

$$2 \sum_{i>0} r_{Ki}^2 \leq \epsilon, \tag{57}$$

for some (small) $\epsilon \geq 0$, [31]. This term is the mean square error (MSE) in $\hat{d}_n$ in Figure 3 in the absence of noise and channel distortion. When $\epsilon = 0$ this constraint is equivalent to self-orthogonality (that is, to g_k being a 'root-Nyquist' filter), but when $\epsilon > 0$ it allows us to trade ISI for other system properties. One of

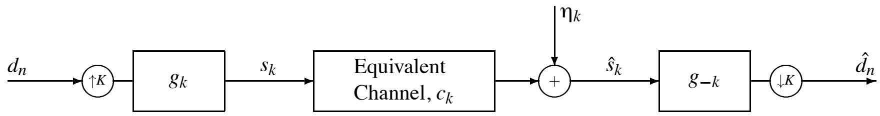

Fig. 3. Equivalent discrete-time model of baseband PAM.

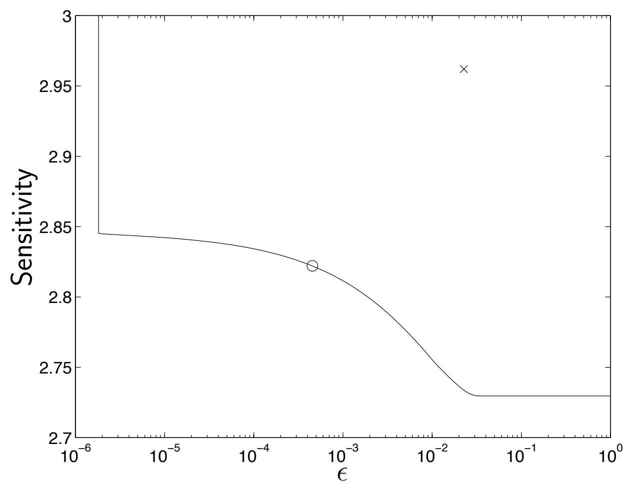

Fig. 4. The trade-off between the sensitivity and ϵ for the IS95 standard for Example 3. The '$\times$' and '$\circ$' denote the positions achieved by the IS95 filter and the robust filter in Figure 5(b), respectively.

these properties might be the sensitivity of the MSE in $\hat{d}_n$ to unknown channel distortion. If the unknown channel is modelled as $c_k = \delta_k + c_k^{(e)}$, where δ_k is the Kronecker delta (which is the impulse response of a distortionless channel), then an appropriate measure of the sensitivity of the PAM scheme is the worst-case MSE over a bounded set of $c_k^{(e)}$'s, [31]. For a given bound ϵ on the ISI, this sensitivity can be minimized by solving Problem 1 with $\tilde{\boldsymbol{x}} = \tilde{\boldsymbol{r}}$, $r_0 = 1$, $\boldsymbol{Q} = \tilde{\boldsymbol{I}}$, $\boldsymbol{l} = \boldsymbol{0}$, and the additional constraint in (57), [31].

Example 3: The filter specified for the synthesis of the chip waveform in IS95 has length 48 and $K = 4$ and satisfies the spectral mask specified in the standard (and illustrated in Figure 1), but it generates a large MSE in a distortionless channel. To efficiently determine whether this MSE can be reduced whilst simultaneously reducing the sensitivity to unknown channel distortion, the modified version of Problem 1 was solved for various values of ϵ. (Each solution was obtained in about 23 seconds.) The trade-off is shown in Figure 4, from which it is clear that the IS95 filter can be greatly improved upon. The spectra of the IS95 filter and a representative optimal filter are plotted in Figure 5. The robust filter provides a substantially lower 'chip error rate' than the IS95 filter in a slowly-varying frequency-selective Rician fading channel, as shown in Figure 6. (See [31] for the details.) $\square$

Example 4: In addition to tradeoffs between ISI and sensitivity, tradeoffs between ISI and bandwidth are also of interest in the design of PAM schemes. For a given level of ISI, a filter achieving the minimum

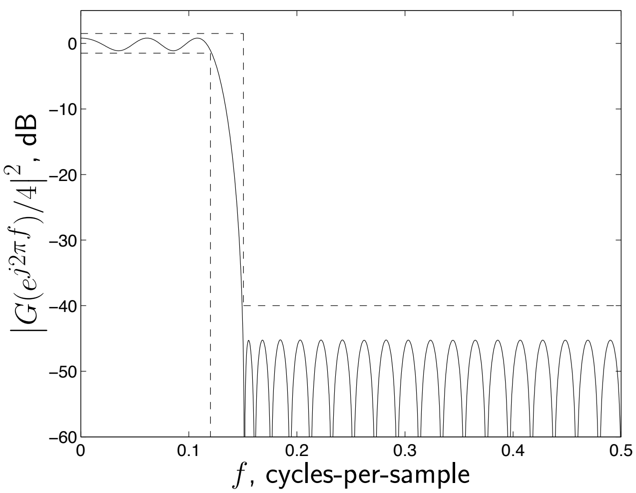

(a) IS95 filter, length 48.

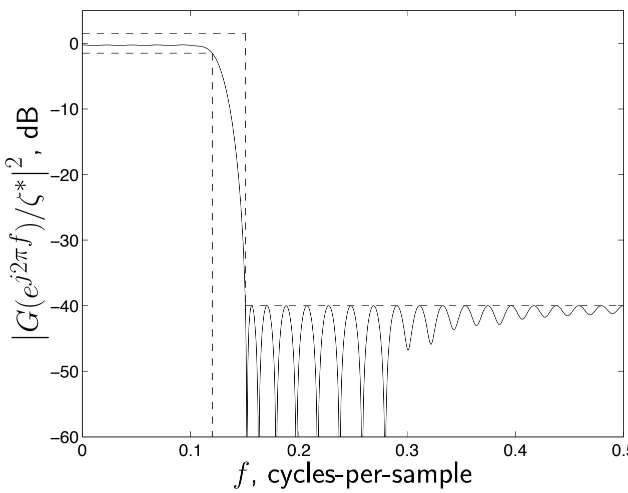

(b) Robust filter, length 48.

Fig. 5. Power spectra (in decibels) of the filters in Example 3, with the IS95 mask. Here, ζ^* is the optimal value of ζ from the modified version of Problem 1.

bandwidth can be efficiently found using a bisection-based search on the stop-band edge of the mask for the feasibility boundary of a convex cone feasibility problem [31]. That feasibility problem is based on the modified version of Problem 1 used in Example 3. (This is a variation of the method used to find minimum bandwidth self-orthogonal filters in [10].) The resulting tradeoff for the IS95 spectral mask is plotted in Figure 7, from which it is clear that the IS95 filter is some distance from the optimal filters. □

B. Beamformer Design

In standard narrowband beamforming applications, the outputs of each antenna element at a given instant are linearly combined to form the array output at that instant [32]. If $x_k(n)$ denotes the complex envelope of the output of the kth antenna element at the nth instant, and if $y(n)$ denotes the complex envelope of the array output at that instant, then

$$y(n) = \boldsymbol{x}(n)^{\mathrm{T}}\boldsymbol{w} = \boldsymbol{w}_c^{\mathrm{H}}\boldsymbol{x}(n),$$

where w_k is the 'weight' applied to the output of the kth antenna element, and $[\boldsymbol{w}_c]_k = \bar{w}_k$. It is well known [32] that if the array geometry is linear, with equi-spaced elements with separation d, and if the array operates on signals with wavelength λ, then the (complex) 'gain' of the array for a signal arriving at an angle ϕ to broadside (perpendicular to the array) is

$$\tilde{W}(\phi) = e^{\mathrm{j}\chi}W(e^{\mathrm{j}2\pi(d/\lambda)\sin\phi}),$$

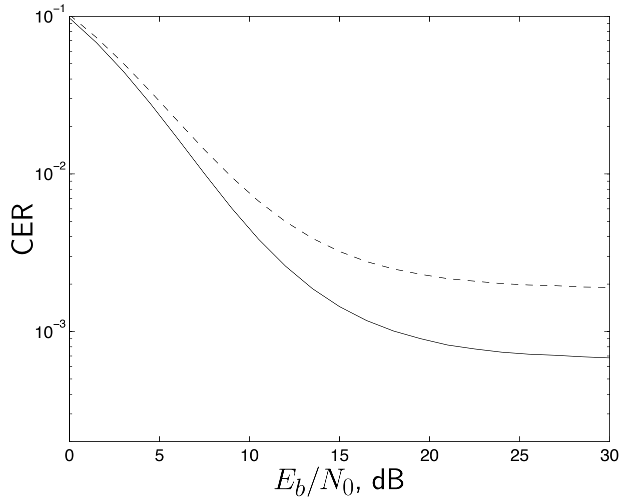

Fig. 6. Simulated chip error rates (CER) in a slowly-varying frequency-selective Rician channel against signal-to-noise ratio for Example 3. Legend—Dashed: IS95 filter; Solid: robust filter.

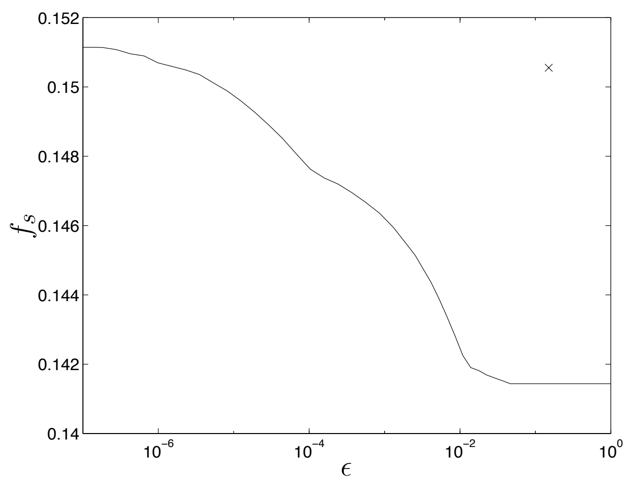

Fig. 7. Minimal stop-band edge f_s against ISI bound ϵ for the IS95 mask. The '×' denotes the position of the IS95 filter.

where $W(e^{j\theta})$ is the Fourier Transform of w_k, and $e^{j\chi}$ determines the 'phase centre' of the array. For simplicity, we will focus on the standard case where $d = \lambda/2$.

In many applications, we would like to control the 'beam pattern' of the array, $|\tilde{W}(\phi)|^2$, but that results in non-convex constraints on w_k. Using the autocorrelation of the weights, $r_m = \sum_k w_k \bar{w}_{k-m}$, we have that $\tilde{R}(\phi) = \sum_m r_m e^{-jm\pi \sin\phi} = |\tilde{W}(\phi)|^2$, and therefore bound constraints on $|\tilde{W}(\phi)|^2$ result in linear constraints on r_m. For an M-element array,

$$\tilde{R}(\phi) = \operatorname{Re} \boldsymbol{v}(\pi \sin\phi; M-1)^{\mathrm{H}} \tilde{\boldsymbol{I}} \tilde{\boldsymbol{r}},$$

where $[\tilde{\boldsymbol{r}}]_m = r_m$, $0 \le m \le M-1$ and $\tilde{\boldsymbol{I}}$ was defined in Section V–A. Therefore, piecewise constant and

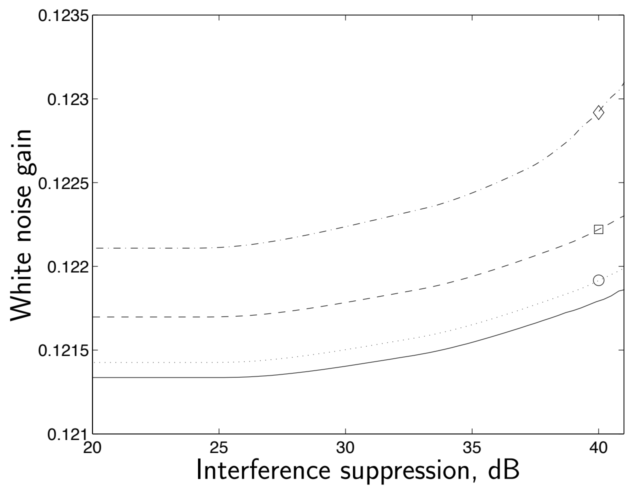

Fig. 8. The trade-off between the minimum white noise gain $\boldsymbol{w}^{\mathrm{H}}\boldsymbol{w}$, and the interference suppression $|\Delta_i|$, for maximum sidelobe levels, Δ_s, of 0.1 dB (solid), -18 dB (dotted), -20 dB (dashed), and -22 dB (dot-dashed) for Example 5. The $\circ$, $\square$ and $\diamond$ denote the trade-offs achieved by the beamformers in Figure 9.

piecewise trigonometric polynomial constraints on $|\tilde{W}(\phi)|^2$ can be compactly enforced in an analogous way to that for the spectral masks in Section V–A, as we now demonstrate in a simple example derived from [32, Figure 2.5].

Example 5: Suppose that a desired signal impinges on a 16-element linear equi-spaced array with element separation $d = \lambda/2$ from an angle of $\phi_d = -18° \pm 6°$, and that interfering signals arrive from angles in the range $\phi_i = 21.5° \pm 6°$. An interesting data independent [32] beamforming problem is to minimize the response to (spatially) white noise (i.e., $\boldsymbol{w}^{\mathrm{H}}\boldsymbol{w} = r_0$), subject to the gain in the direction of the desired signal being within $\pm\Delta_d$ dB, and to the gain in the direction of the interferers being less than Δ_i dB. Furthermore, to guard against unexpected interferers from other directions, we would like to keep the sidelobes below Δ_s dB, and to constrain the main lobe (as determined by Δ_s) to be within $-18° \pm 13°$. In short, our objective is to minimize the white noise gain, subject to a mask of the shape in Figure 9, below. This problem can be cast in a similar way to Problem 1 with $\tilde{\boldsymbol{x}} = \tilde{\boldsymbol{r}}$, $\zeta = 1$, $\boldsymbol{Q} = \boldsymbol{0}$, and $\boldsymbol{l} = -\boldsymbol{e}_0/2$, except that the vector $\tilde{\boldsymbol{r}}$ and the various $\boldsymbol{X}$ and $\boldsymbol{Z}$ matrices may be complex. Therefore, the trade-offs between the white noise gain and the level of interference suppression, for different values of the maximum sidelobe level and for a 'look direction ripple' with $\Delta_d = 0.1$ dB can be efficiently found. They are presented in Figure 8. Examples of the resulting beam patterns are shown in Figure 9. (Each optimal $\tilde{\boldsymbol{r}}$ was computed in about seven seconds.) These examples clearly demonstrate the role which the sidelobe level constraint plays in determining the shape of the beam pattern. $\square$

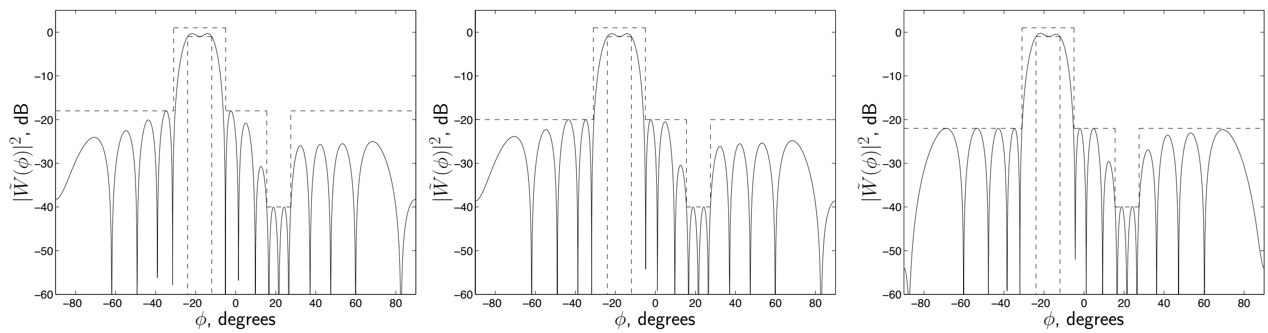

(a) $\Delta_s = -18$ dB.

(b) $\Delta_s = -20$ dB.

(c) $\Delta_s = -22$ dB.

Fig. 9. Beam patterns with minimal white noise gain, subject to 40 dB interference suppression and different maximum sidelobe levels, Δ_s, for Example 5, along with the corresponding masks.

VI. Concluding Remarks

In this paper, we have provided a compact representation of piecewise constant and piecewise trigonometric polynomial spectral mask constraints via linear matrix inequalities. This representation is precise and avoids the heuristic approximation of the mask incurred when discretization techniques are used. The representation is also convex, and it generates practically competitive design algorithms (based on well-established interior point methods) for a diverse class of FIR filtering and narrowband beamforming problems. Using such algorithms, (in)feasibility of the spectral mask can be detected reliably, which is especially important when the design problem is solved iteratively in a binary search scheme (such as in minimal length filter design). In addition to these applications, generalizations of our results to rational filters (i.e., infinite impulse response filters) and to multidimensional filters are of interest in control theory, as well as signal and image processing, and are currently being pursued. In closing, we point out that we have efficiently solved the design problems which result from our compact representation (e.g., Problem 1) using a sophisticated, but general purpose, convex cone programme solver [26]. Although this is convenient from a practitioner's perspective, we believe that more efficient implementations of our design approach can be obtained by developing an application specific solver which exploits the extensive algebraic structure which our design problems possess. Recent work on application specific solvers for problems from the same class [33, 34] suggests that the resulting reductions in computational and memory requirements can be substantial.

Acknowledgment. The third author would like to thank Professor Yu. Nesterov for sharing his ideas and for stimulating research in this area.

References

[1] T. W. Parks and C. S. Burrus, *Digital Filter Design*, J. Wiley & Sons, New York, 1987.

[2] K. Steiglitz, T. W. Parks, and J. F. Kaiser, "METEOR: A constraint-based FIR filter design program", *IEEE Trans. Signal Processing*, vol. 40, no. 8, pp. 1901–1909, Aug. 1992.

[3] I. W. Selesnick, M. Lang, and C. S. Burrus, "Constrained least square design for FIR filters without specified transition bands", *IEEE Trans. Signal Processing*, vol. 44, no. 8, pp. 1879–1892, Aug. 1996.

[4] J. W. Adams and J. L. Sullivan, "Peak-constrained least-squares optimization", *IEEE Trans. Signal Processing*, vol. 46, no. 2, pp. 306–321, Feb. 1998.

[5] P. Leister and T. W. Parks, "On the design of digital FIR filters with optimum magnitude and minimum phase", *Arch. El. Übertr.*, vol. 29, pp. 270–274, 1975.

[6] O. Herrmann and W. Schuessler, "Design of nonrecursive digital filters with minimum phase", *Electronics Letters*, vol. 6, no. 11, pp. 329–330, 28 June 1970.

[7] X. Chen and T. W. Parks, "Design of optimal minimum phase FIR filters by direct factorization", *Signal Processing*, vol. 10, pp. 369–383, June 1986.

[8] S.-P. Wu, S. Boyd, and L. Vandenberghe, "FIR filter design via semidefinite programming and spectral factorization", in *Proc. IEEE Conf. Decision Control*, 1996, pp. 271–276.

[9] S.-P. Wu, S. Boyd, and L. Vandenberghe, "FIR filter design via spectral factorization and convex optimization", in *Applied and Computational Control, Signals, and Circuits*, B. Datta, Ed., vol. 1. Birkhauser, Boston, May 1999.

[10] T. N. Davidson, Z.-Q. Luo, and K. M. Wong, "Design of orthogonal pulse shapes for communications via semidefinite programming", *IEEE Trans. Signal Processing*, vol. 48, no. 5, pp. 1433–1445, May 2000.

[11] T. N. T. Goodman, C. A. Micchelli, G. Rodriguez, and S. Seatzu, "Spectral factorization of Laurent polynomials", *Adv. in Comp. Math.*, vol. 7, no. 4, pp. 429–454, 1997.

[12] R. Hettich and K. O. Kortanek, "Semi-infinite programming: Theory, methods and applications", *SIAM Review*, vol. 35, no. 3, pp. 380–429, Sept. 1993.

[13] P. Moulin, M. Anitescu, K. O. Kortanek, and F. A. Potra, "The role of linear semi-infinite programming in signal adapted QMF bank design", *IEEE Trans. Signal Processing*, vol. 45, no. 9, pp. 2160–2174, Sept. 1997.

[14] O. Rioul and P. Duhamel, "A Remez exchange algorithm for orthonormal wavelets", *IEEE Trans. Circuits Systems—II*, vol. 41, no. 8, pp. 550–560, Aug. 1994.

[15] H. H. Dam, K. L. Teo, S. Nordebo, and A. Cantoni, "The dual parameterization approach to optimal least square FIR filter design subject to maximum error constraints", *IEEE Trans. Signal Processing*, vol. 48, no. 8, pp. 2314–2320, Aug. 2000.

[16] B. D. O. Anderson, K. L. Hitz, and N. D. Diem, "Recursive algorithm for spectral factorization", *IEEE Trans. Circuits Systems*, vol. CAS–21, no. 6, pp. 742–750, Nov. 1974.

[17] B. Hassibi, A. H. Sayed, and T. Kailath, *Indefinite-Quadratic Estimation and Control: A Unified Approach to H^2 and H^∞ Theories*, SIAM, Philadelphia, 1999.

[18] P. P. Vaidyanathan, "The discrete-time Bounded-Real Lemma in digital filtering", *IEEE Trans. Circuits and Systems*, vol. CAS–32, no. 9, pp. 918–924, Sept. 1985.

[19] J. E. Marsden, *Basic Complex Variables*, W. H. Freeman and Company, San Francisco, 1973.

[20] A. V. Oppenheim and R. W. Schafer, *Discrete-Time Signal Processing*, Prentice Hall, Englewood Cliffs, NJ, 1989.

[21] A. A. Markov, "Lecture notes on functions with the least deviation from zero", 1906, Reprinted in *A. A. Markov, Selected Papers*, N. Achiezer, Ed., pp. 244–291, GosTechIzdat, Moscow, 1948 (in Russian).

[22] Lukacs, "Verscharfung der ersten mittelwertsatzes der integralrechnung fur rationale polynome", *Math. Zeitschrift*, vol. 2, pp. 229–305, 1918.

[23] V. Powers and B. Reznick, "Polynomials that are positive on an interval", Technical Report, University of Illinois at Urbana-Champaign, 1998. To appear in *Trans. Amer. Math. Soc.*.

[24] Yu. Nesterov, “Squared functional systems and optimization problems”, in *High Performance Optimization*, H. Frenk, K. Roos, T. Terlaky, and S. Zhang, Eds., pp. 405–440. Kluwer Academic Publishers, Dordrecht, The Netherlands, 2000.

[25] Yu. Nesterov and A. Nemirovsky, *Interior Point Polynomial Algorithms in Convex Programming*, SIAM, Philadelphia, 1994.

[26] J. F. Sturm, Using SeDuMi 1.02, a MATLAB toolbox for optimization over symmetric cones. *Optimization Methods and Software*, 11–12:625–653, 1999. See `http://fewcal.kub.nl/sturm/software/sedumi.html` for updates.

[27] L. Vandenberghe and S. Boyd, “Semidefinite programming”, *SIAM Review*, vol. 31, no. 1, pp. 49–95, Mar. 1996.

[28] M. S. Lobo, L. Vandenberghe, S. Boyd, and H. Lebret, “Applications of second-order cone programming”, *Lin. Algebra Applics*, vol. 284, no. 1–3, pp. 193–228, Nov. 1998.

[29] Y. Ye, *Interior Point Algorithms: Theory and Analysis*, J. Wiley & Sons, New York, 1997.

[30] “Proposed EIA/TIA interim standard. Wideband spread spectrum digital cellular system dual-mode mobile station-base station compatibility standard”, Technical Report TR45.5, QUALCOMM, Inc., San Diego, CA, Apr. 1992.

[31] T. N. Davidson, “Efficient design of waveforms for robust pulse amplitude modulation based on mean square error criteria”, In *Proc. X European Signal Processing Conf.*, Tampere, Finland, Sept. 2000.

[32] B. D. Van Veen and K. M. Buckley, “Beamforming: A versatile approach to spatial filtering”, *IEEE Acoust., Speech, Signal Processing Mag.*, pp. 4–24, Apr. 1988.

[33] Y. Genin, Y. Hachez, Yu. Nesterov, and P. Van Dooren, “Convex optimization over positive polynomials and filter design”, In *Proc. UKACC Int. Conf. Control.*, Cambridge, U.K., Sept. 2000.

[34] B. Alkire and L. Vandenberghe, “Interior point methods for magnitude filter design”, In *Proc. Int. Conf. Acoust., Speech, Signal Processing*, Salt Lake City, IT, May 2001.